Preservation of Last Interglacial and Holocene transgressive systems tracts in the Netherlands and its applicability as a North Sea Basin reservoir analogue

Peeters, J.; Cohen, K. M.; Thrana, C.; Busschers, F. S.; Martinius, A. W.; Stouthamer, E.; Middelkoop, H.

DOI
10.1016/j.earscirev.2018.10.010

Publication date
2019

Document Version
Final published version

Published in
Earth-Science Reviews

Earth-Science Reviews 188 (2019) 482–497

Contents lists available at ScienceDirect

Earth-Science Reviews

journal homepage: www.elsevier.com/locate/earscirev

Preservation of Last Interglacial and Holocene transgressive systems tracts in the Netherlands and its applicability as a North Sea Basin reservoir analogue

J. Peeters[a,b,c,*], K.M. Cohen[a,b,c], C. Thrana[d], F.S. Busschers[b], A.W. Martinius[d,e], E. Stouthamer[a], H. Middelkoop[a]

[a] Department of Physical Geography, Faculty of Geosciences, Utrecht University. Princetonlaan 8a, P.O. Box 80.115, 3508 TC, Utrecht, The Netherlands
[b] TNO – Geological Survey of the Netherlands, Princetonlaan 6, P.O. Box 80.015, 3508 TA, Utrecht, The Netherlands
[c] Deltares, Unit Subsurface and Groundwater systems, Daltonlaan 600, 3584 BK, Utrecht, The Netherlands
[d] Equinor ASA, Arkitekt Ebbells veg 10, 7053 Trondheim, Norway
[e] Faculty of Civil Engineering and Geosciences, Delft University of Technology, Stevinweg 1, P.O. Box 5048, 2600, GA, Delft, The Netherlands

ARTICLE INFO

Keywords:
Facies proportion
Estuary
Incised-valley fill
Sequence stratigraphy
Eemian interglacial
Åre Formation
River Rhine

ABSTRACT

Understanding of complex sedimentary records formed by transgressive systems is critical for hydrocarbon exploration and exploitation, and carbon capture and storage. This paper discusses the facies proportions and preservation of the Last Interglacial and Holocene transgressive systems tracts in the Netherlands and their applicability as a North Sea Basin analogue for the Early Jurassic Åre Formation in the Norwegian offshore. New and existing data from both (sub-)modern transgressive Rhine records were thoroughly reviewed from a sequence stratigraphic perspective, before volumetrics were calculated and longitudinal trends quantified at reservoir scale.

Large differences between the Last Interglacial and Holocene transgressive systems were found: the volume of fluvial deposits is almost six times larger and the volume of organics nearly twenty times larger in the Holocene record than in the Last Interglacial record. In contrast, the volume of estuarine deposits in the Holocene record is only half of that of the Last Interglacial record. Remarkably, both records show similar averaged sediment-trapping rates of 8–9 km^3/ka. Initial valley configuration and relative sea-level rise-rates during both transgressions were key controls on the volume and spatial arrangement of the transgressive deposits. Relative sea-level fall and river avulsion determined what amount of sediment was left preserved after completion of one interglacial-glacial cycle.

Comparison of the Late Quaternary Rhine records with the Late Triassic to Early Jurassic Åre Formation in the Heidrun Field off mid-Norway, showed the potential of the (sub-)modern Rhine records as analogues for ancient stratigraphic records. Especially the transgressive Rhine sequence from the Last Interglacial provided remarkable similarities in facies proportions, preservability, autogenic processes and controlling forcings, ranging from metre-scale vertical-successions to kilometre-scale field-wide events for parts of the Åre Formation. The side-by-side availability of the truncated Last Interglacial and (still) fully preserved Holocene transgressive system proved to be an excellent natural laboratory to study the stratigraphic architecture and assess depositional trends and preservability over longer time scales (> 100 ka). It nevertheless demonstrates that no 'one-size-fits-all' analogue exists, but that various other analogues are needed to solve the complex puzzle which the Åre Formation resembles.

1. Introduction

Transgressive sequences are highly heterogeneous units that make up a significant part of sedimentary basins, where they function as sequence stratigraphic marker horizons. They represent complex stratigraphic environments; their internal sedimentary architecture is a product of fluvial, estuarine and shallow marine-processes that alternated rapidly in space and time in response to allogenic controls (e.g. sea-level rise, (glacio-)tectonics, climate change) and autogenic processes (e.g. avulsion) (e.g. Dalrymple, 2006; Stouthamer et al., 2011; Blum et al., 2013; Miall, 2016). Understanding transgressive sequences is critical for hydrocarbon exploration and exploitation (e.g. Cattaneo

* Corresponding author.
E-mail address: j.peeters1.uu@gmail.com (J. Peeters).

https://doi.org/10.1016/j.earscirev.2018.10.010
Received 26 January 2018; Received in revised form 28 September 2018; Accepted 9 October 2018
Available online 15 October 2018
0012-8252/

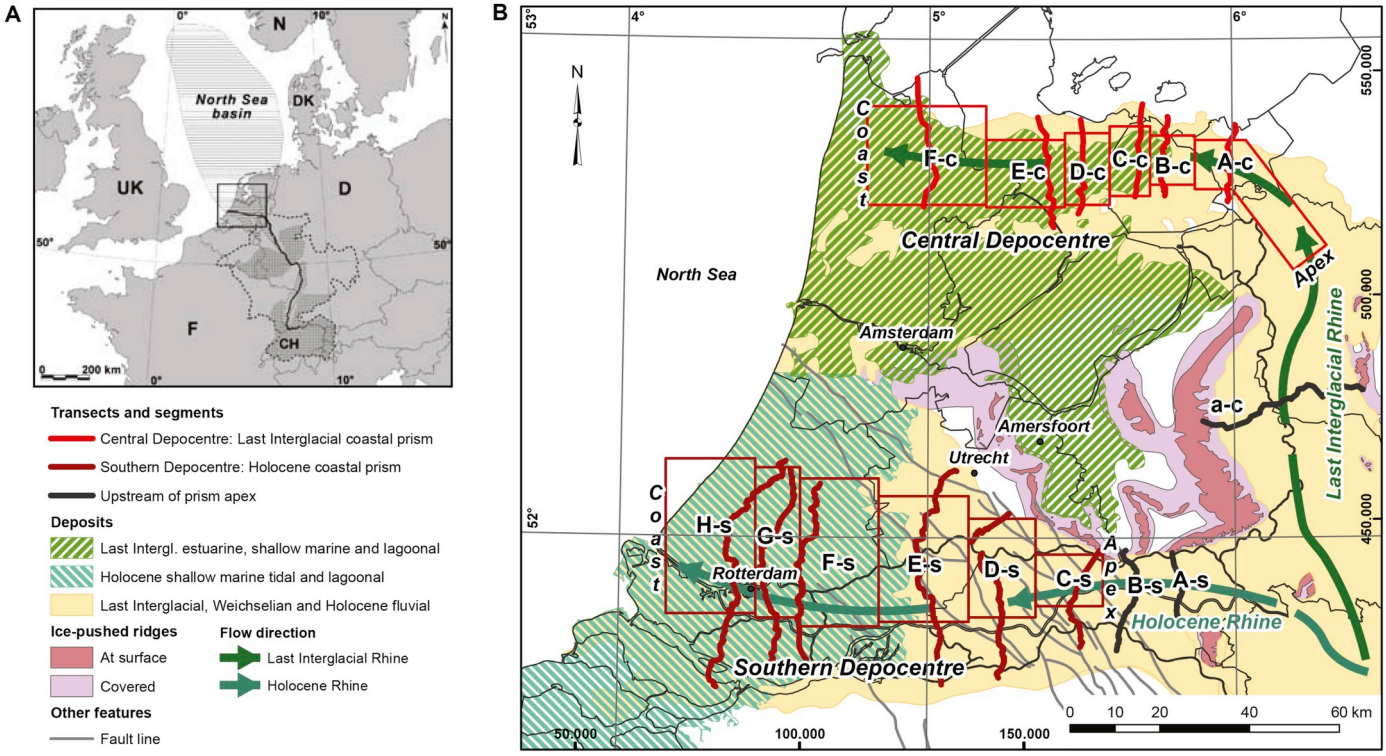

Fig. 1. A) Map showing north-western Europe with the present Rhine drainage-basin positioned at the southern margin of the tectonically subsiding North Sea Basin and the study area in the Netherlands. B) Detailed map of the study area showing the Last Interglacial (or Eemian interglacial) and Holocene coastal prism deposits in the central and southern Netherlands respectively in relation to the inherited Saalian glacial topography (after Peeters et al., 2016 with map data from TNO-GSN, 2016). Transects A-c to F-c are from Peeters et al. (2016). Transect a-c is from Busschers et al. (2007) and Peeters et al. (2015). Transects A-s to E-s are from Gouw and Erkens (2007); extended from Berendsen (1982), Törnqvist (1993) and Cohen (2003). Transects F-s to H-s are from Hijma et al. (2009).

and Steel, 2003; Martinius et al., 2005; Bjørlykke et al., 2010; Messina et al., 2014) and carbon capture and storage (e.g. Bachu, 2008; Haszeldine, 2009; Hangx et al., 2015), since they control important reservoir characteristics (e.g. sand-body connectivity, reservoir porosity and permeability). However, obtaining quantitative insights in these sequences is often difficult due to common erosional, faulting and compaction processes, and a limited availability of data.

In reservoir geological applications one tends to overcome this by implementing analogue insights derived from for example outcrop studies (e.g. Leren et al., 2010; Martinius and Gowland, 2011; Martinius and Van den Berg, 2011; Ahokas et al., 2014; Howell et al., 2014; Aschof et al., 2018), and cores and seismic logs of buried hydrocarbon reservoirs (e.g. Kjærefjord, 1999; Martinius et al., 2001; Kombrink et al., 2007; Thrana et al., 2014). Another way is to use Quaternary analogues, most-often Holocene systems, for which well-accessible and well-dated information exists, and architecture and heterogeneity can be quantified and understood in higher detail. Yet for modern analogues, it remains challenging to upscale observations of local facies and sediment characteristics to quantitative summaries at reservoir scale.

Translation of highly-detailed young analogue examples (e.g. Hijma et al., 2009) to ancient stratigraphy is complicated, amongst others, by over-preservation of the top sets of modern systems which in ancient reservoir counter examples tend not to preserve. Also the transgressive sequences underneath such top sets have in modern systems not yet experienced full post-depositional erosion. Last Interglacial sequences hold some promise to overcome these over-preservation problems, as they went through one full cycle of interglacial-glacial sea-level oscillation, climate change and crustal movement (e.g. Blum and Törnqvist, 2000; Blum et al., 2013; Bentley et al., 2016), i.e. 4th-order icehouse cycles cf. Haq et al. (1988). Otherwise, Last Interglacial records are still within practical range of high-density data collection and dating control, although admittedly at less fine resolutions as to which the Holocene systems are resolvable. They are suitable for drawing space-time resolved sedimentary analogies, as they are the next-youngest after the Holocene, and because sea-level and climatic history (base level fall, glacial-interglacial regime changes) over the last cycles are nowadays fairly well understood, both regionally and globally (e.g. Brewer et al., 2008; Dutton and Lambeck, 2012; Barlow et al., 2018).

The subsurface of the Netherlands, fed by the river Rhine, hosts both such well-studied Last Interglacial (e.g. Van Leeuwen et al., 2000; Peeters et al., 2015, 2016; Sier et al., 2015), and Holocene transgressive sedimentary records (e.g. Hijma and Cohen, 2011; Stouthamer et al., 2011). These two records are each trapped in their own separate palaeovalley, owing to developments during the penultimate and the last glacial low-stand respectively (e.g. Cohen et al., 2002; Törnqvist et al., 2000, 2003; Wallinga et al., 2004; Busschers et al., 2005, 2007, 2008; Hijma et al., 2012; Peeters et al., 2016). The two transgressive systems have formed under largely similar hinterland conditions (i.e. interglacial forested) and only subtly differing marine conditions (Long et al., 2015; Peeters et al., 2015, 2016). The side-by-side availability of a truncated Last Interglacial and a more fully preserved Holocene transgressive system, opens a promising natural laboratory to assess its sedimentary architecture, depositional trends and preservability over longer time scales (> 100 ka).

In this study, the Rhine's Last Interglacial and Holocene transgressive records were used to quantify longitudinal facies trends at reservoir scale. A method was developed to deal with post-depositional overprint and setting differences, to quantify facies proportions and intercompare the two records. Trends seen in the records were assessed and the representativeness of the results as a hydrocarbon reservoir analogue evaluated by comparing these (sub-)modern systems with transgressive sequences in the Jurassic Åre Formation reservoir in the Norwegian offshore (Båt Group: Dalland et al., 1988; Thrana et al., 2014).

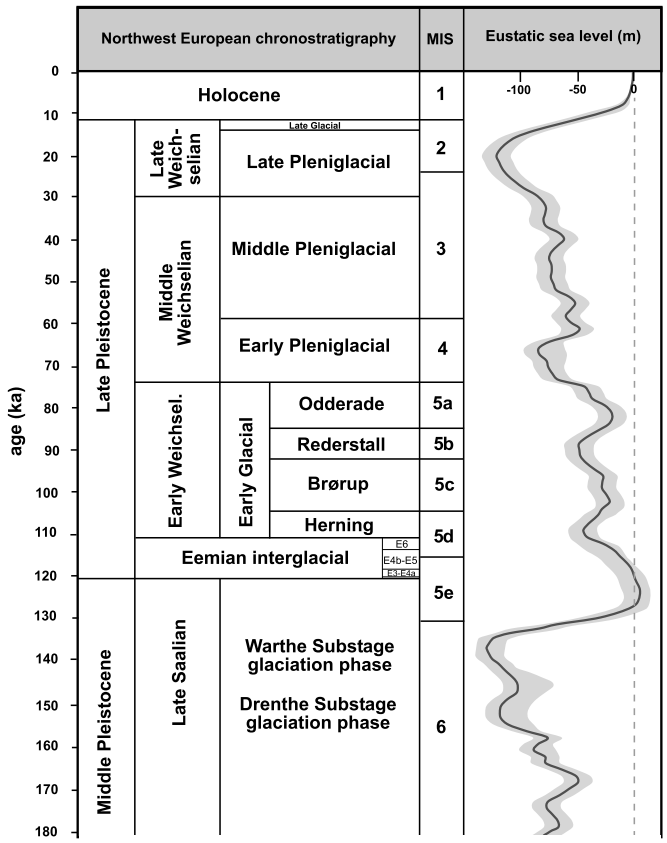

Fig. 2. Chronostratigraphic chart comprising the Northwest European subdivision of the late Quaternary (after Busschers et al., 2007; Peeters et al., 2015) updated with the latest insights regarding the timing of the Eemian in NW Europe (from Sier et al., 2015; Peeters et al., 2016). The composite eustatic sea-level curve (dark grey line) and associated confidence interval (light grey area) is from Waelbroeck et al. (2002) with adjustments after Medina-Elizalde (2013). Eemian pollen assemblage zones (PAZs) are indicated (cf. Zagwijn, 1961, 1996): the short 500-year interval of PAZs E1-E2 is not visualised. Correlations with the marine isotope record are based on Bassinot et al. (1994).

2. Geological setting and sequence stratigraphic framework

The Netherlands is positioned at the southern margin of the tectonically subsiding Cenozoic North Sea basin (Fig. 1) (Ziegler, 1994; Van Balen et al., 2005). During the Middle and Late Pleistocene, the northern part of this basin was repeatedly glaciated, which for the River Rhine in the south resulted in large-scale drainage re-arrangements (e.g. Busschers et al., 2008; Hijma et al., 2012). In the Late Pleistocene (i.e. Marine Isotope Stage (MIS) 2–5: Fig. 2), fluvial deposition in the Netherlands was largely controlled by a northwest-southeast oriented series of ice-pushed ridges (e.g. Van den Berg and Beets, 1987), that were inherited from the Saalian glaciation which terminated shortly before (mid-MIS 6), and that divided the study area into the Central and Southern Depocentres (Peeters et al., 2015, 2016). A Northern Depocentre of early Middle Pleistocene age also exists (Busschers et al., 2008), but was terminated during the Saalian glaciation. The Central Depocentre hosted the estuary of the Rhine system during the Eemian, as the Last Interglacial is called in north-western Europe, whereas the Southern Depocentre hosted the Rhine river mouth during the middle Holocene (Fig. 1; Fig. 2). This paper subdivides the lower Rhine record of the last two interglacial-glacial cycles adopting depositional sequence terminology after Haq et al. (1987, 1988) and Posamentier et al. (1988). In translating and applying such terminology to the Last Interglacial and Holocene sedimentary architecture, Hijma and Cohen (2011) was followed.

At about 190 km offshore on the Mid-Norwegian Shelf (Fig. 3), circa 2700 m below the Norwegian Sea, ancient estuarine-deltaic depositional settings exist in the Late Triassic to Early Jurassic Åre Formation (Fig. 4; Dalland et al., 1988; Thrana et al., 2014). The Åre Formation, within the Båt Group, has been identified in several hydrocarbon fields on the Halten Terrace. The Heidrun Field (16 × 8 km: Fig. 3), where the formation is about 670 m thick and represents c. 13 Ma, is regarded characteristic for the Åre depositional system (Thrana et al., 2014). The Åre Formation has an overall transgressive nature (Kjærefjord, 1999; Thrana et al., 2014), reflecting the gradual tectonic development (i.e. 2nd to 3rd-order greenhouse-type cycle cf. Haq et al., 1988) of the Halten Terrace Basin during development of the North Atlantic rift system in the early Jurassic (Marsh et al., 2010).

2.1. Netherlands' Central Depocentre: Last Interglacial Rhine

The sedimentary fill of the east-west oriented incised Rhine-valley in the Central Depocentre holds a c. ~50 m thick and 10-20 km wide record that basically consists of three stacked successions (Fig. 5). The lower part of the valley fill, bounded by a basal erosive contact that functions as the sequence boundary (SB), holds an (upper) lowstand systems tract (LST), comprised of coarse-grained deposits of the latest Saalian (late MIS 6) braided-style river Rhine (Unit S6: Table A1), with a top set of medium-grained sands with clay and organic-mixtures, of a latest Saalian and early-Eemian (MIS 5e; Pollen Assemblage Zones (PAZs) E1 and E2 cf. Zagwijn, 1961, 1996) meandering-style river (Unit A1: Table A1) (Peeters et al., 2016). Next, a coastal prism succession is encountered, partly bounded by a transgressive surface (TS). It consists of fine-grained floodbasin sediments of the transgressive sequence (Unit A2), which changes into estuarine deposits towards its top (Unit M1), comprising the Last Interglacial partially filled, wave-dominated Rhine estuary where four depositional sub-environments were distinguished (Fig. 5). Units A2 and M1 together form the wedge-shaped transgressive systems tract (TST: Table A1), which was rapidly built-up in only 1.5 ka, and ended during PAZ E4a (cf. Zagwijn, 1961, 1996: Fig. 2). In this period, sea-level rose from −35 to −15 m MSL (Zagwijn, 1983), implying a rate of RSL rise of 13 m/ka (Fig. 5). Younger fluvial erosion has largely truncated the Last Interglacial sequence, making that only along the northern valley rim a rare patch of the Eemian highstand systems tract (HST) has been preserved and identified. Here, the maximum flooding surface (MFS) is found at −19.2 m MSL (Sier et al., 2015; Peeters et al., 2016). HST formation lasted approximately 5 ka (i.e. PAZs E4b-E5 cf. Zagwijn, 1961, 1996), during which RSL reached its highstand maximum at −8 m MSL in the south of the Central Depocentre (Zagwijn, 1983), implying an average relative sea-level rise-rate of 7 m/ka (Fig. 5). Next, a last succession representing the falling stage systems tract (FSST) is encountered, comprised of coarse-grained fluvial deposits (Units A3 and A5: Table A1) dating from the Early and Middle Weichselian (MIS 3-5d). This systems tract truncated the HST and top of the TST of the Last Interglacial coastal prism succession. Preservation of the FSST was decided when the Rhine abandoned the valley and the Central Depocentre starting c. 60 ka and completed around 38 ka BP, after which sedimentation only occurred by small local rivers and aeolian activity (Busschers et al., 2007; Peeters et al., 2016). See Appendix B for further details.

2.2. Netherlands' Southern Depocentre: Holocene Rhine

The Holocene coastal prism is c. ~20-25 m thick at the coast and stretches far inland (Fig. 6). Its lower 14-19 m comprise the TST; the upper 5-6 m accommodate the HST. Architectural reconstructions show onlap from 9.5 ka onwards (Hijma et al., 2009; Vos et al., 2015), beginning with terrestrial stages of fluvial overbank aggradation and Basal Peat formation (upper LST unit: Fig. 6; Table A2). Thereafter, transgression occurred (cf. Hijma and Cohen, 2011), registered as subaqueous deposits (TS and TST: Fig. 6; Table A2). The depositional

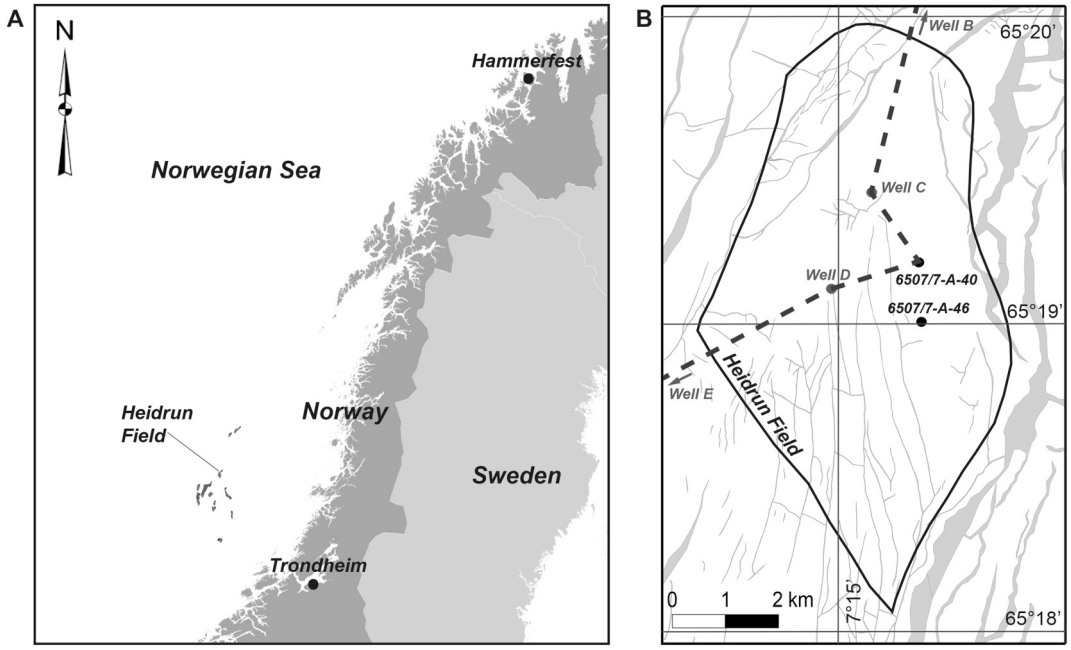

Fig. 3. A) Location of the Heidrun hydrocarbon field on the Halten Terrace, off Mid-Norway in the Norwegian Sea. B) Detailed map showing the Heidrun Field, its fault-structure, the location of wells 6507/7-A-40 and 6507/7-A-46, and the approximate position of the longitudinal transect (dashed line).

contact marking the TS is in the seaward half of the TST developed as an upper-estuarine, freshwater-tidal clayey-gyttja. This facies grades upwards into increasingly saline central, lower and outer estuarine subaqueous tidal muds, dissected by sand-mud tidal channel systems. In the very west, where the coastal-zone barrier-complex formed, mud-containing sandy facies mark a ravinement surface (RS) at the transition to foreshore and beach-barrier deposits (Fig. 6). Landwards, the TST is primarily developed as upper-estuarine subaqueous fresh-water tidal environments (Hijma and Cohen, 2011; Bos and Stouthamer, 2011), reaching as far upstream as transect E-s (Fig. 1; Fig. 6). The MFS in the Holocene coastal prism is associated with a matured beach-barrier system and hence more-protected back-barrier conditions, by 6.3–6.0 ka leading to widespread peat formation (Fig. 6) (Hijma and Cohen, 2011; Koster et al., 2017; De Haas et al., 2018). The Holocene TST thus resembles 2.5 ka (from 8.5 to 6 ka) when sea-level rose from −20 to −6 m MSL (Hijma and Cohen, 2010), dropping its rate from > 10 m/ka to c. 3 m/ka with an average of c. 6 m/ka. The HST buried both the seaward and the inland parts of the TST. With the transgressive tidal inlet and estuarine systems mostly being silted-up, and the matured barrier complex prograding, fresh-water terrestrial delta plain environments dominated the back-barrier area (Table A2), while in the youngest 3 ka development was increasingly human-impacted (Stouthamer et al., 2011; Vos, 2015; Pierik et al., 2017). See Appendix B for further details.

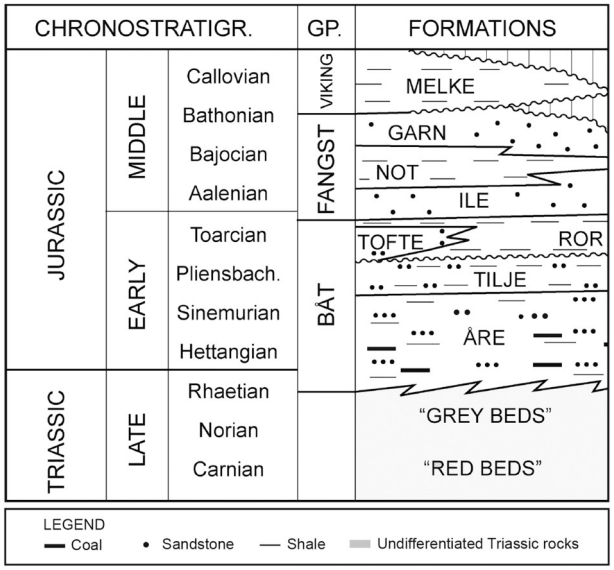

Fig. 4. Chronostratigraphic and lithostratigraphic chart comprising the Triassic-Jurassic succession on the Halten Terrace, off Mid-Norway (modified after Thrana et al., 2014 from Dalland et al., 1988).

2.3. Norwegian Heidrun Field: Late Triassic to Early Jurassic Åre Formation

The basal part of the Åre Formation consists of non-marine coastal plain deposits (Åre reservoir zones (RZs) 1–2) that develop upward through lower-delta plain and brackish-water interdistributary bay deposits (Åre RZs 3–4), through a wide array of wave-influenced estuarine floodbasins with occasionally bay-head delta facies (Åre RZs 5–6), to culminate with marine shoreface deposits (Åre RZ 7) (Thrana et al., 2014). As Åre RZs 5–6 potentially show the highest resemblance with the Last Interglacial and Holocene Rhine systems, these RZs were selected for evaluation and comparison.

At its base, Åre RZ 5.1 is distinguished from the Åre RZ 4 by a heterolithic central-estuary basin mudstone that can be traced across the Heidrun Field and represents a TS (TS2 in Fig. 7) that marks the field-wide shift to the wave-influenced estuarine setting of the Åre RZ 5.1 TST (Thrana et al., 2014). At least 8 upward shallowing successions of genetically related beds, bounded by flooding surfaces, were recognised and ascribed to parasequences (cf. Van Wagoner et al., 1988, 1990): i.e. 5th-order events which group to form 4th-order sequence stratigraphic divisions (Haq et al., 1988; Mitchum and Van Wagoner, 1990). The parasequences show coarsening-upward trends in partially wave-influenced estuarine deposits, and reflect autogenic shifts within the coastal system. Åre RZ 5.1 has a total thickness of 24-30 m and is thought to span an interval of c. 100 ka (Fig. 7; Thrana et al., 2014).

Åre RZ 5.2 is defined by a prominent change in facies into a field-wide belt of more tide-influenced distributary channel sandstones, that partly incised into the underlying Åre RZ 5.1 deposits. This erosional

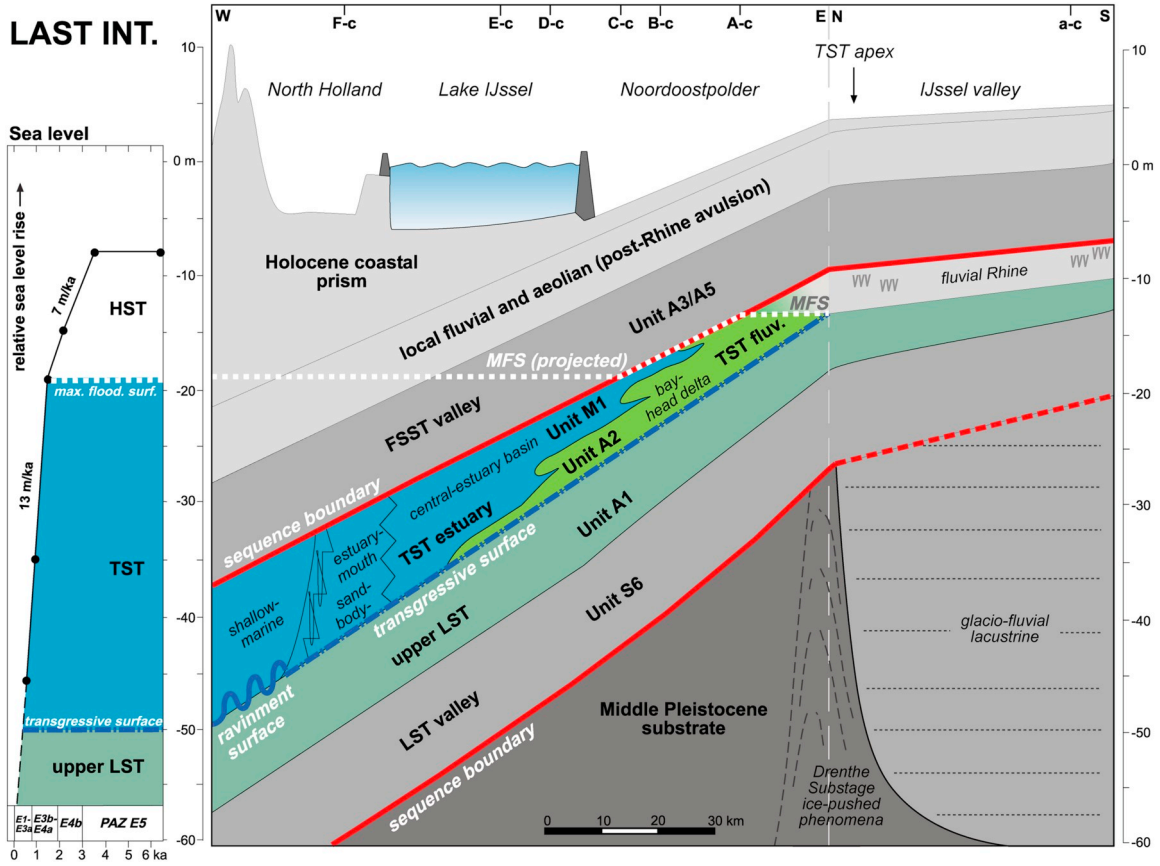

Fig. 5. Schematic longitudinal transect through the central axis of the Netherlands' Central Depocentre, showing the sequence stratigraphy of the incised Rhine-valley fill, with emphasis on the Last Interglacial (or Eemian interglacial) TST, facies distribution and sea-level history (after Peeters et al., 2015, 2016). The Last Interglacial Rhine estuary comprises four depositional sub-environments: 1) a sandy bay-head delta upstream in the valley; 2) a fine-grained, mud-prone central-estuary basin; 3) an estuary-mouth sand-body complex in the outer estuary; and 4) a fine-grained estuary margin along its northern flank. All sedimentary units (Unit S6-A5) are cf. Peeters et al. (2016), the sea-level curve is after Zagwijn (1983, 1996). The position of the geological transects is indicated at the top.

surface is characterised by sub-angular mud clasts as the basal lag of amalgamated tide-influenced channel sandstones, which represent the candidate sequence boundary (c.SB2: Fig. 7) and mark the base of the Åre RZ 5.2 LST. These sediments are partly overlain by subtidal flat facies, which mark the transition to the overlying unit (Fig. 7; Thrana et al., 2014). Åre RZ 5.3 is characterized by two parasequences - dominated by upward-coarsening very-fine to fine sand - which are interpreted as bay-head delta deposits. Åre RZs 5.2 and 5.3 are respectively 9-10 m and 7-9 m thick, and their combined duration is estimated to c. 200 ka (Fig. 7; Thrana et al., 2014).

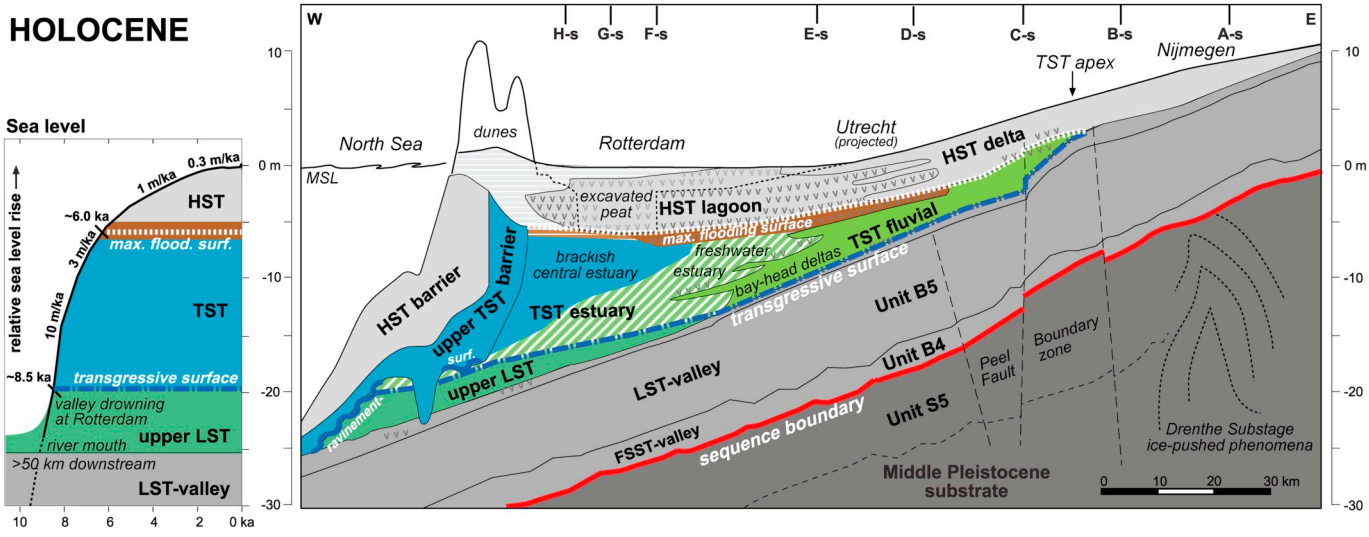

Fig. 6. Schematic longitudinal transect through the central axis of the Netherlands' Southern Depocentre, showing the sequence stratigraphy of the Holocene incised Rhine-valley fill, with emphasis on the TST facies distribution and sea-level history (after Hijma and Cohen, 2010, 2011; Cohen and Hijma, 2014). The position of the geological transects is indicated at the top.

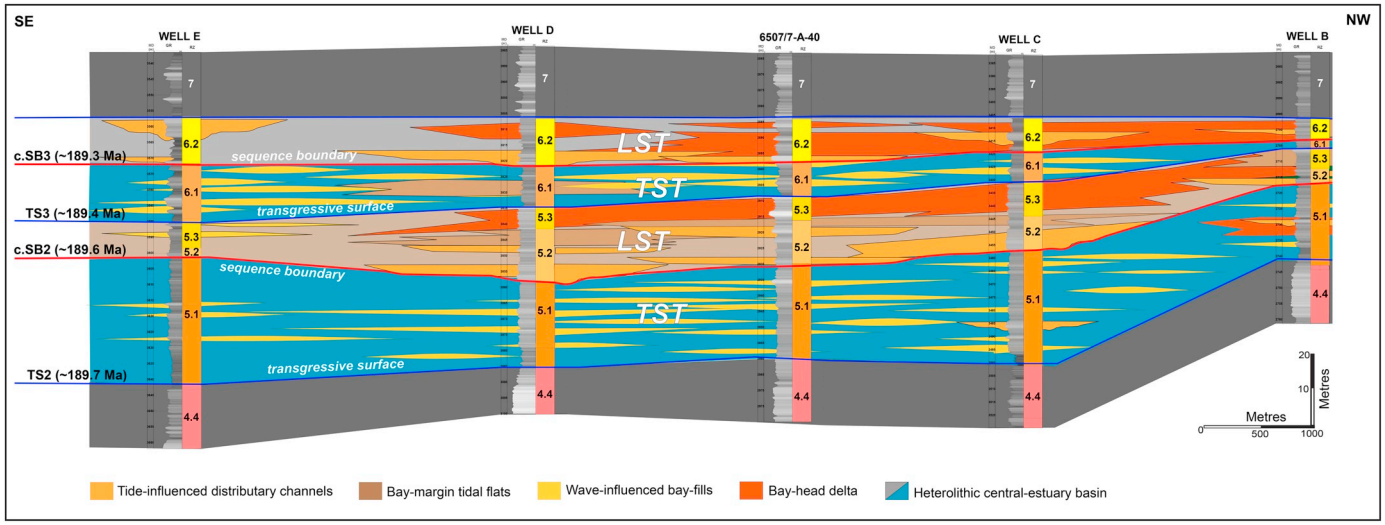

Fig. 7. Schematic longitudinal transect, running down-dip in NW-SE direction across the Heidrun Field, showing vertical and lateral distribution of facies associations and interpreted sequence stratigraphic surfaces within Åre reservoir zones (RZs) 5–6. Interpretations are based on cored intervals and wireline logs. Approximate duration of intervals is based on biostratigraphy (Thrana et al., 2014).

The base of Åre RZ 6.1 is marked by a large-scale transgressive surface (TS3: Fig. 7), which is characterized by estuarine facies, wave-influenced bay-fills and bay-margin tidal flats. These deposits forming 2–3 upward-coarsening parasequences characterize the Åre RZ 6.1 TST. Åre RZ 6.1 is 10-15 m thick and has an estimated duration of c. 100 ka (Fig. 7). A field-wide shift into tide-dominated channels forms the next candidate sequence boundary (i.e. c.SB3) and marks the LST of Åre RZ 6.2. Åre RZ 6.2 has a thickness of 13-15 m and an estimated duration of c. 100 ka (Fig. 7; Thrana et al., 2014). See Appendix B for further details.

3. Materials and methods

3.1. Data collection

Underlying this study is the data from two sets of valley-wide geological transects slicing the Last Interglacial (Peeters et al., 2016) and Holocene Rhine records (stepwise developed in: Törnqvist, 1993; Cohen, 2003; Busschers et al., 2007; Gouw and Erkens, 2007; Gouw and Berendsen, 2007; Hijma et al., 2009). In the Central Depocentre seven transects dissect the late Middle to Late Pleistocene incised-valley fill, whereof six (A-c to F-c) hold the Last Interglacial TST (Fig. 1). In the Southern Depocentre, eight transects dissect the Late Pleistocene to Holocene incised-valley fill, of which six (C-s to H-s) hold the Middle Holocene TST (Fig. 1). Detailed information on research methods, sequence descriptions and dating control is found in Berendsen and Stouthamer (2000), Gouw and Erkens (2007), Hijma et al. (2009) and Peeters et al. (2016).

Well data from the Åre Formation provided a third dataset used in this study. Circa 77 wells penetrate the Åre Formation in the Heidrun Field, but only 18 reach the lowermost parts. Fifteen wells have cored intervals from the Åre formation (1362 m of cored length in total) and allow for detailed sedimentological and ichnological description (Thrana et al., 2014). For this study, the log data from wells 6507/7-A-40 and 6507/7-A-46 (Fig. 3) were used in particular because together they cover almost the entire Åre Formation (i.e. RZs 2 to 7.2) in 210 m cored length. Information on the research methods, more detailed descriptions of the sedimentary record and their stratigraphic division scheme are found in Thrana et al. (2014).

3.2. Depocentre areal segmentation

To come to a longitudinal segmentation for the two depocentres, the segmentation of Erkens and Cohen (2009) of the Holocene coastal prism was taken over, and the approach adopted for segmentation of the Last Interglacial. Criteria for segmentation of the Holocene coastal prism had been (i) the location of the cross-valley transects (i.e. one section per segment) and (ii) similarity of areal facies distribution proportions to cross-section determined facies proportions (Fig. 1). For the Last Interglacial dataset, the second criterion was hard to assess objectively, and hence the Central Depocentre segment boundaries were put halfway each successive transect (Fig. 1). In defining the width of the Southern and Central Depocentre segments for comparison of the TST stages, cross-valley segment width was taken as the mapped width of the incised valleys.

3.3. Preserved and eroded volume quantification

Based on TST area and thickness information compiled for the two cases (Table A1; Table A2), the preserved volume was calculated by multiplying each segment's mean TST thickness with its area. For the Last Interglacial record, in segments D-c to F-c also the pre-FSST truncated TST volume was estimated, replacing actual preserved thickness with a conservatively reconstructed mean-thickness. For this, the mean depth of basal transgressive sediments in the respective transects and the highest known occurrence of the Last Interglacial TST observed in segment C-c at −19.2 m MSL (core Rutten: Sier et al., 2015; Peeters et al., 2016) were used. To reconstruct the eroded volume of the Last Interglacial HST in segments A-c to F-c (Table A1) a similar approach was followed. For this calculation, a maximum height of the HST in core Rutten was determined at a depth of circa -12 m MSL. See Appendix B for more details regarding the preserved and eroded volume quantification.

3.4. Volumetric deposit proportion calculation

Volumetric proportions of deposit associations for the two cases were quantified using cross-valley transects and earlier mapping. Following Holocene studies by Gouw (2008), Erkens (2009) and Hijma et al. (2009), five classes were used: 1) FCD: Fluvial coarse-grained deposits, comprising channel-belt and crevasse sands; 2) FFD: Fluvial fine-grained deposits: overbank floodplain clays and silts; 3) OR: Organics: peat and gyttja; 4) ECD: Estuarine coarse-grained deposits, which comprise the basal barrier/estuary-mouth sand-body, estuarine distributary channels, and bay-head delta sands; and 5) EFD: Estuarine

fine-grained deposits: fine-grained central-estuary sediments. For each class, the TST cross-sectional area per transect was calculated and multiplied by the segment's east-west length, yielding volumes per class per segment. Deposit proportions were then obtained by dividing these volumes by the total segment volume.

3.5. TST apex and coastline definition

To properly intercompare the Last Interglacial and Holocene TSTs, it is important to define equivalent up- and downstream limits of both coastal prisms. This was done by first slicing the coastal prisms following sequence stratigraphic principles (i.e. TS and MFS recognition), and thereafter performing a volumetric assessment, to point out the apex and coastline positions at the time of the MFS. The TST-apex was recognised as a marked increase in preserved TST-accommodated volume, thickening in downstream direction. This is at x = 225 km (Netherlands coordinate system) for the Last Interglacial (Fig. 5) and x = 168 km for the Holocene sequence (Fig. 6). A marked drop in preserved volume in estuarine facies indicates the position of the transgressive-coastline. It is found at x = 115 km in the Last Interglacial and x = 70 km in the Holocene sequence. This made that in the Central Depocentre the reach from segment A-c up-to and including F-c, and in the Southern Depocentre the reach from segment C-s up-to and including H-s were selected for cross-comparison. For the deposit proportion cross-comparisons among the systems, absolute distances along the apex-coast transects of each system were normalised by division by the system's apex-coast distance.

3.6. Åre Formation quantification

To quantify deposit proportions for the Åre RZs 5–6 TSTs, classes of deposits comparable to the Last Interglacial and Holocene TST analysis were used. Deposit proportions were calculated based on wells 6507/7-A-40 and 6507/7-A-46. Since only point well-data were available, no information regarding deposit volumes could be obtained for the Åre Formation. Based on this calculation, Åre reservoir zones with coarse-grained and fine-grained deposits comparable to those found in the Last Interglacial and Holocene TSTs were selected for further comparison. For this purpose, a more detailed subdivision on facies-association level was made, and deposit proportions were determined for each facies association.

4. Results

4.1. Deposit proportions, volumes and trends in the Last Interglacial TST

The preserved volume of the Last Interglacial wedge-shaped TST totals 9.0 km^3 (Fig. 8A). Estuarine deposits (ECD + EFD: 7.2 km^3) make up 80% of it, fluvial deposits only account for 19% (1.7 km^3). Coarse-grained deposits – i.e. facies of estuarine inlets and distributary channels – comprise 33% (ECD + FCD: 3.0 km^3) while fine-grained deposits – i.e. facies of estuarine and fluvial floodbasins – dominate the record volumetrically (66%; 5.9 km^3). Only 1% of the volume – at the present state of burial and consolidation – is from organics (0.1 km^3). An additional volume of later-eroded TST was estimated to equal about 5.0 km^3 (see Section 3.3). The Last Interglacial HST has hardly been preserved. A volume of 7.0 km^3 is estimated to have been eroded, downstream of the TST apex (Fig. 8A).

Coarse- and fine-grained fluvial facies (FCD resp. FFD) dominate the inland part of the TST. In segment A-c these amount 85% of 0.8 km^3, while the remaining 15% are organics (OR). This is the only segment of the Last Interglacial TST where organics make up a substantial part of the coastal prism. Fluvial deposits are present in segments A-c to D-c (1.7 km^3 in total), with fairly constant proportions: some 11% FCD and 25–35% FFD, the remainder being coarse- and fine-grained estuarine facies (ECD resp. EFD). Further downstream in segments E-c and F-c, fluvial deposits hardly occur. The preserved estuarine deposits in these segments totals 6.0 km^3, with coarse-grained facies being relatively abundant. The central and inland parts of the TST estuary, i.e. segments B-c to D-c, accommodate a further 1.2 km^3, with fine-grained central basin facies dominating (EFD between 50 and 70%). ECD is virtually absent in segments D-c and C-c, but picks up inland in segment B-c (20%: Fig. 8B-C), where it is regarded to represent bay-head delta environments (Peeters et al., 2015, 2016).

Considering longitudinal trends in total coarse-grained proportions (i.e. TCD: FCD and ECD proportions combined), relatively high values of 30% and 45% are encountered at the upstream and downstream ends of the Last Interglacial TST (Fig. 8D). In the central estuarine segments (C-c, D-c), a minimum TCD proportion of 12% occurs. Because organic volume plays no significant role in the Last Interglacial TST, the total proportion of fines (i.e. TFD: FFD and EFD proportions combined) mirrors the TCD values. The average TCD proportion for the Last Interglacial TST is 25%, where the average TFD proportion is 72%.

In the fluvial part, a key feature is the drop in FFD versus a relatively constant low FCD in the inland-central parts of the system in segments B-c to D-c (Fig. 8D). Estuarine fines (EFD) and coarse deposits (ECD) covary differently. EFD increases rapidly in downstream direction from central segment C-c onwards to maxima of 60–70%, whereas ECD only does this in the most downstream reach (segment F-c and arguably E-c).

After a c. 70 ka period of regressive conditions due to RSL lowering, and associated channel incision, only a relatively thin (5–10 m) unit of the transgressive sediments has been preserved (Fig. 5). The particular succession of events that took place during the Late Pleistocene, resulted in the removal of a significant part (i.e. 12 km^3 of the TST and HST: Fig. 8A) of the Last Interglacial coastal prism. Only 9 km^3, or about 45% of the total volume (21 km^3) did preserve. This volume is almost entirely made up by the TST: the HST is nearly completely eroded.

4.2. Deposit proportions, volumes and trends in the Holocene TST

The wedge-shaped volume of the Holocene TST, measures 19.9 km^3 (Fig. 9A). Fluvial deposits contribute 50% (10.1 km^3) and, estuarine deposits 40% (8 km^3). Organics (1.8 km^3) comprise 10% of the TST at the present state of burial and consolidation. This last percentage is high in TST context, but considerably smaller than the proportion of organics in the HST, in which peats are laterally more extensive and much less consolidated (Fig. 6; Gouw, 2008; Erkens et al., 2016). Coarse-grained deposits make up 33% (6.6 km^3), and fine-grained deposits 58% (11.5 km^3) of the total. The volume of estuarine coarse-grained deposits (ECD) is larger than that of the fluvial coarse-grained deposits (FCD).

Going from the TST apex in a downstream direction, over the first 40 km (from segment C-s to E-s), the Holocene coastal prism rapidly widens and thickens (segment volumes increase from 0.2 to 2.2 km^3). This upstream part of the TST consists in majority of fluvial facies (over 65%; at the TST apex 90%: Fig. 9B-C). The remaining non-estuarine TST volume consists of organics (Fig. 6; see also Van der Woude, 1984; Törnqvist, 1993). Organic proportions peak at 35% in segments D-s and E-s, but that remarkably high value occurs over a short distance of the total coastal prism length. In the segments further downstream (F-s to H-s), where brackish estuarine deposits overlying freshwater-tidal and fluvial-lacustrine facies are encountered, the OR proportion rapidly drops to 5%. Estuarine deposits amount to 60% of 5.5 km^3 total volume in the most downstream segment (H-s) and reach only slightly lower proportions in the other downstream segments G-s and F-s, where coarse-grained estuarine facies (ECD) dominates estuarine fines (EFD). Of the fluvial deposits across segments F-s to H-s, the coarse-grained versus fine-grained proportions are fairly constant (FFD proportion: 45%; FCD proportion: 10%) and amount for roughly half (i.e. 8 km^3) of the total segment volumes.

In the Holocene TST, total coarse-grained proportions (TCD) show a

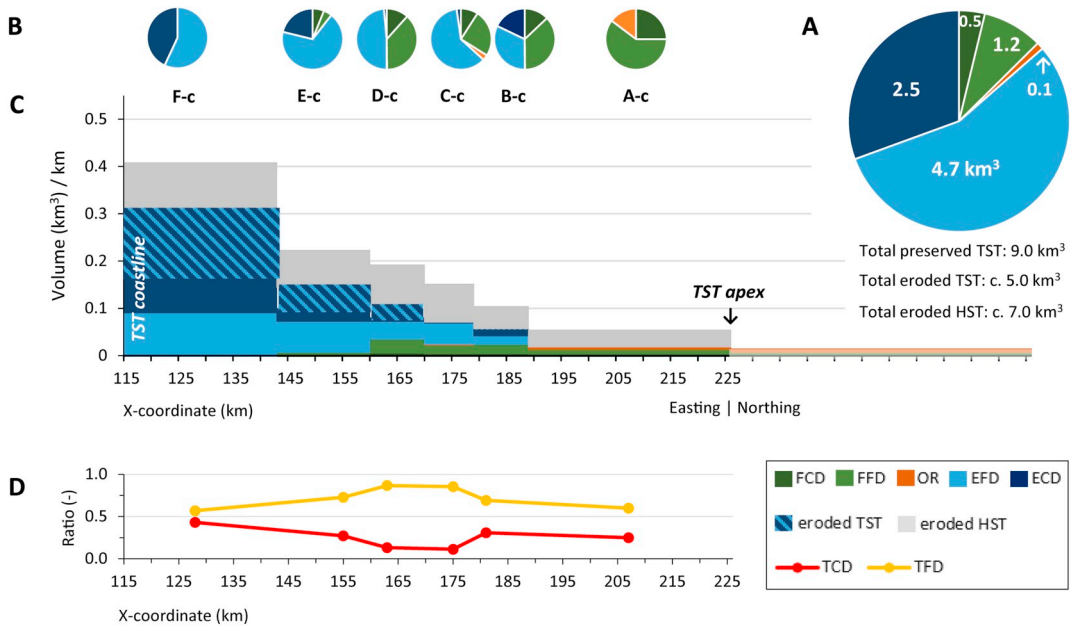

Fig. 8. Volumes and deposit proportions in the Last Interglacial TST. A) Large circle chart shows the proportions of the entire system and cumulative total volumes of the different deposits in the Last Interglacial TST. B) Circle charts show the preserved deposit proportions per segment. C) Bar diagram shows the *volume-per-kilometre*, cumulating in the total volume per segment. The volume of eroded Last Interglacial transgressive deposits is indicated with the alternating blue diagonal stripes. The volume of the eroded HST is indicated in grey. D) Line diagram shows the TCD and TFD ratios.

gentle increase in downstream direction, from 15% upstream to about 40% in the most downstream segment (Fig. 9D). In between, segments D-s and E-s show a minimum value of just above 10%. The system-averaged TCD proportion is 25%. The high TCD values in the downstream part result from the abundant ECD occurrence, in this case estuarine sand. In the upstream segments, TCD is exclusively fluvially sourced (FCD). Because volumes of organics are also in play in the Holocene TST, the longitudinal trends in TFD do not simply mirror the TCD. The TFD proportion reaches an average value of 0.6 and is fairly constant: 51–75% (Fig. 9D). If the trade-off between EFD and FFD is considered, a contrast is observed. The proportion of FFD decreases from about 75% to 35% in a downstream direction (segment C-s to H-s), while EFD compensates for that loss in line with increased ECD.

4.3. Comparison of Last Interglacial and Holocene TSTs

Comparison of the TST volumes from the Last Interglacial (including the 'later eroded' volumes; Fig. 8A) and Holocene (Fig. 9A), firstly

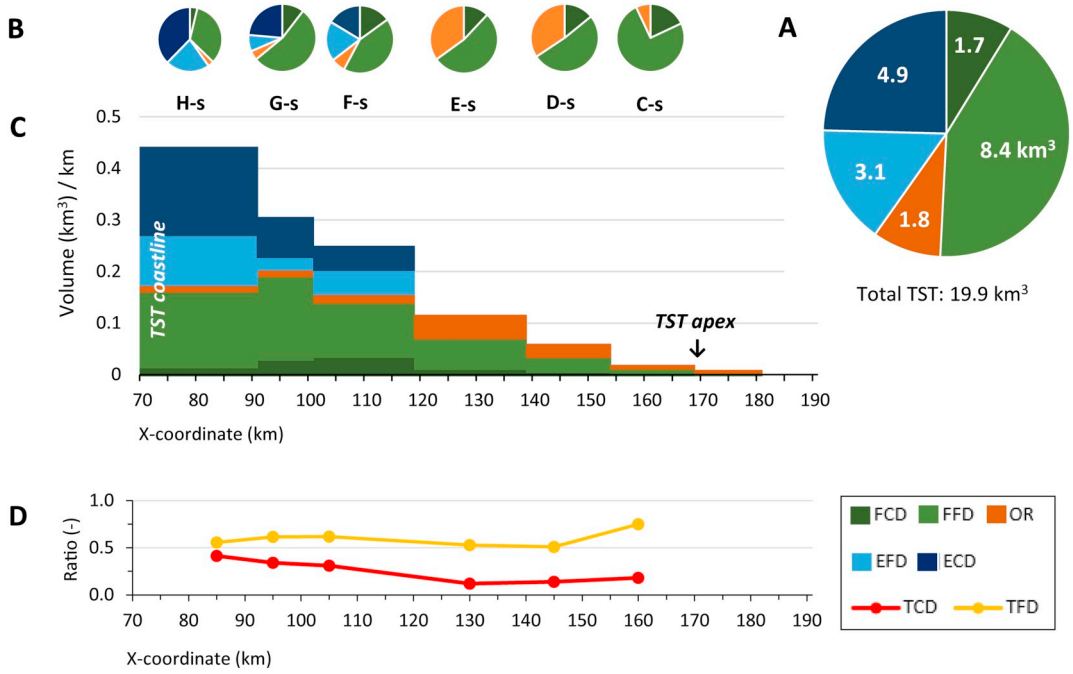

Fig. 9. Volumes and deposit proportions in the Holocene TST. A) Large circle chart shows the proportions of the entire system and cumulative total volumes of the different deposits in the Holocene TST. B) Circle charts show the deposit proportions per segment. C) Bar diagram shows the *volume-per-kilometre*, cumulating in the total volume per segment. D) Line diagram shows the TCD and TFD ratios.

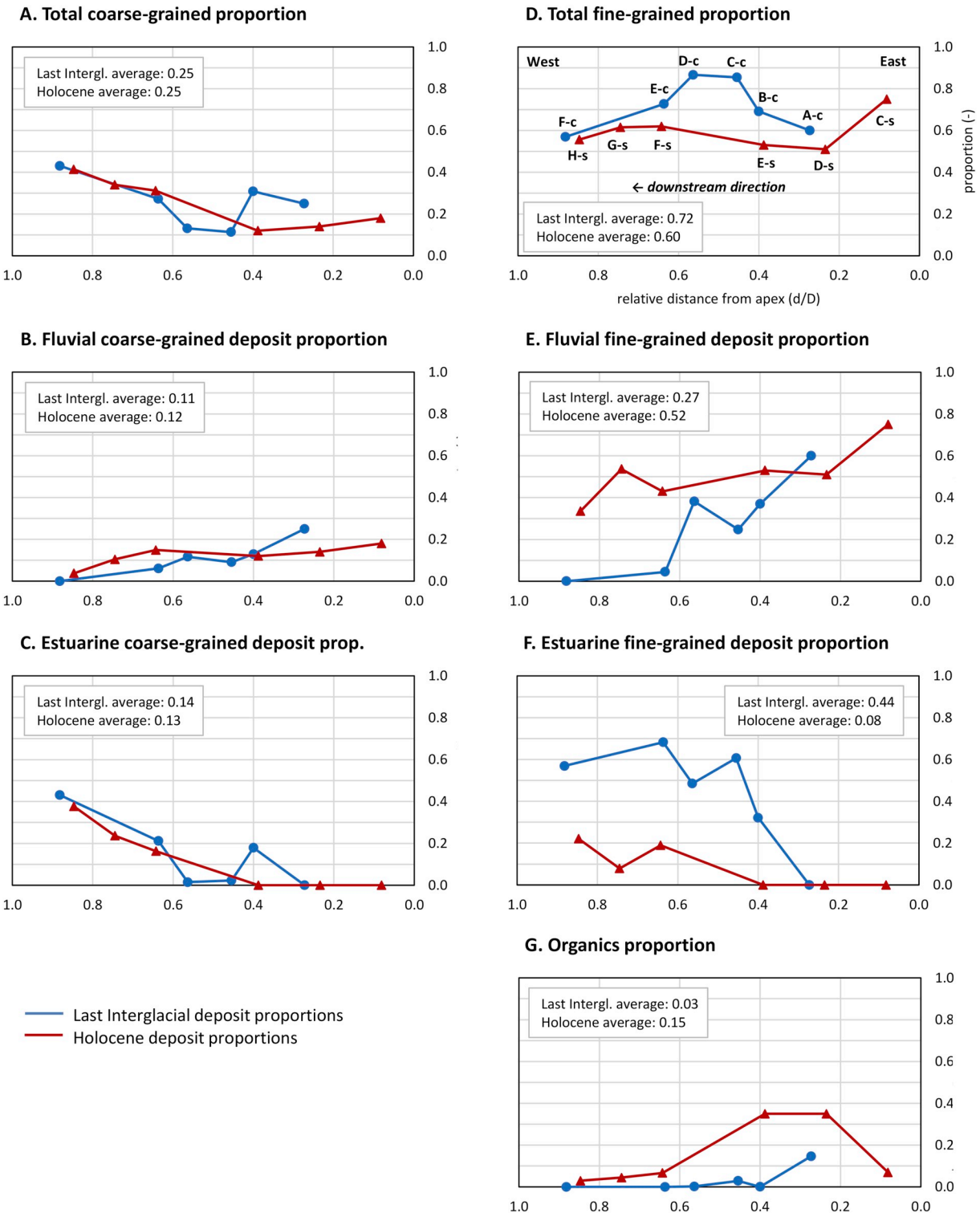

Fig. 10. Comparison between the preserved Last Interglacial and Holocene TSTs for: A) Total coarse-grained proportion (TCD); B) Fluvial coarse-grained deposit proportion (FCD); C) Estuarine coarse-grained deposit proportion (ECD); D) Total fine-grained proportion (TFD); E) Fluvial fine-grained deposit proportion (FFD); F) Estuarine fine-grained deposit proportion (EFD); and G) Organics proportion. The distance is given as the relative distance from the apex (relative distance d/D: with d = downstream distance from apex, and D = total distance between apex and coastline) in order to normalize the distance over the horizontal-axis. The relative position of the Last Interglacial and Holocene transects are shown in panel D.

reveals a difference in total volume: 14 km^3 for the Last Interglacial versus 20 km^3 for the Holocene TST. When dividing these volumes by the time span over which they formed (see Sections 2.1 and 2.2), the resulting bulk sediment-trapping rates appear to be similar: 9 km^3/ka in the Last Interglacial and 8 km^3/ka in the Holocene.

The proportions of estuarine, fluvial and organic facies differ strongly between the two systems (Fig. 5 vs. Fig. 6; Fig. 8 vs. Fig. 9). The Holocene TST holds a six times larger volume of fluvial deposits (10.1 km^3) than the Last Interglacial TST (1.7 km^3). The volumetric proportion of organics in the Holocene sequence is almost 20 times as

high as in the Last Interglacial sequence. In the Last Interglacial TST, organics occur only in the upstream reaches, implying that the volumetric differences are not just caused by consolidation with increased burial depth. The accommodation of estuarine facies between both TSTs differs too: 8.0 km^3 in the 2500-yr Holocene record versus 12.2 km^3 in the 1500-yr Last Interglacial record.

The TCD proportions in both systems show however similar trends, with maximum values being reached at their most downstream ends. For both systems, the overall TCD proportion is 25% (Fig. 10A). Particularly the trends in FCD proportions are similar, with an almost identical average of 11–12% (Fig. 10B). On closer inspection, the trends in TCD proportions do however differ: a discrepancy exists in the near absence of ECD in the central part of the Last Interglacial TST (Fig. 10C).

The TFD proportions of both systems show more differences than the TCD. A distinct maximum in TFD proportions is found in the central part of the Last Interglacial system, whereas the Holocene TFD trend is not that discriminative (Fig. 10D). The FFD proportions of the Last Interglacial transgressive system show a downstream decreasing trend, while the FFD proportions of the Holocene system are more constant (Fig. 10E). Hence a larger amount of fluvial fine-grained sediments is present in the more downstream and central parts of the Holocene system, when compared to the Last Interglacial system. The EFD proportions differ strongly too. Where the EFD proportions of the Last Interglacial system rapidly increase in downstream direction to a maximum value, the Holocene system only shows a small increase much farther downstream (Fig. 10F). Apparently, a much larger proportion of estuarine fine-grained sediment is present in the Last Interglacial than in the Holocene system.

4.4. Deposit proportions and trends in the Åre RZs 5–6

Analysis of deposit proportions within Åre RZs 5–6 shows that ECD in general dominate the sedimentary record of this interval of the Åre Formation with proportions as high as 95% (Åre RZ 6.2: Fig. 11). Organics (OR) only make up for 1% of the volume in Åre RZ 5.3. Because this value is not corrected for compaction, it will likely underestimate the original proportion of organics in the system. The proportions of estuarine fine-grained deposits (EFD) are in general relatively low in Åre RZs 5–6; they only dominate in Åre RZ 5.1 with a proportion of 60% (Fig. 11), while another substantial proportion of 46% is found in Åre RZ 6.1. These relatively high proportions of EFD are comparable to those found in the downstream parts of both Last Interglacial and Holocene TSTs, making these reservoir zones of particular interest for further comparison.

The quantification of deposit proportions for the Åre RZ 5.1 TST provides data for three different facies associations: wave-influenced bay-fills, heterolithic central-estuarine basin and crevasse splay (see Appendix B for details). The proportions of wave-influenced bay-fills and heterolithic central-estuarine basin in the sedimentary record of Åre RZ 5.1 are similar (c. 49%), whereas the contribution of crevasse splay is small (1%: Fig. 11B). Both wave-influenced bay-fills and heterolithic central-estuarine basin associations have their own distinctive deposit proportions (Fig. 11B). The wave-influenced bay-fill sediments are a mixture of ECD (63%) and EFD (37%), while the heterolithic central-estuarine basin sediments only consist for 15% of ECD, and are dominated by EFD (85%). Within the minor facies association crevasse splay, coarse-grained sediments are dominant over the fine-grained fraction, comprising 85% versus 15% of the volume respectively (Fig. 11B).

Nearly all studied Åre reservoir zones are coarser-grained than the Last Interglacial and Holocene sequences (Fig. 12), except for Åre RZ 5.1 which is its thickest considered TST (Fig. 7). The sedimentary composition of Åre RZ 5.1 shows most similarity with the seaward-most segments of the Quaternary TSTs (Last Interglacial segment F-c: Fig. 8; Holocene segment H-s: Fig. 9). Arguably, the TCD/TFD ratio in Åre RZ 6.1 comes close in resembling the Quaternary TSTs too (Fig. 12), although this RZ shows a somewhat more TCD dominated composition. It should be noted that Åre RZ 6.1 reflects a stronger tidal influence and contains coarser material (Thrana et al., 2014). For all non-TST Åre RZs the TCD/TFD ratio differs distinctly (Fig. 12), greatly dominated by coarse-grained sediments, as would most FSST and LST Quaternary units do.

5. Discussion

5.1. Forcings and boundary conditions: differences between the Rhine TSTs explained

Initial palaeovalley morphology has strongly controlled fluvial and estuarine deposition in both the Last Interglacial and Holocene Rhine systems (e.g. Hijma and Cohen, 2011; Peeters et al., 2015, 2016). Last Interglacial river channels before transgression (upper LST), and the river mouth at the end of transgression (i.e. TST apex), occupied incised-valley inherited positions (Fig. 1). The Last Interglacial TST apex found itself in a relative deeper incised and farther inland-position, and with only modest extent of fresh-water tidal and bay-head delta deposits (Fig. 5), than in the equivalent situation in the Holocene (Fig. 6). The Holocene coastal prism, positioned in the Southern Depocentre closer to the North Sea basin rim, filled a shallower palaeovalley reach in a relatively protruded position (Busschers et al., 2007, 2008; Hijma and Cohen, 2011). The combined initial morphology and base level control (i.e. palaeovalley slope, substrate, background subsidence and inundation depths), in the Holocene case allowed a TST coastal barrier system to initiate (Hijma et al., 2010) that matured while the HST commenced (Beets and Van der Spek, 2000; Beets et al., 2003; De Haas et al., 2018). The Last Interglacial system does not convincingly show Rhine mouth coastal barriers (Peeters et al., 2016), likely due to the morphological difference in combination with high RSL rise-rates resulting in a shorter transgression duration.

The average RSL rise-rate for the Last Interglacial TST was substantially higher (13 m/ka), than that for the Holocene equivalent (6 m/ka). This high rate of RSL rise resulted in rapid increase in accommodation space in the incised Rhine-valley, transforming it into estuarine reaches (Peeters et al., 2016). This environmental change largely affected the deposition of sediments transported by the interglacial Rhine River: while fluvial supply of sediments from upstream continued, sedimentation shifted to the unfilled micro-tidal wave-dominated estuary. The lower averaged rates of sea-level rise for the Holocene TST resulted in a slower drowning of late LST terrain and more extensive provision of accommodation space (Hijma and Cohen, 2011). This allowed the river Rhine to partially keep-up with the transgression for a time, resulting in the deposition of its sediments in a fluvial floodbasin environment instead of that of an estuary, which explains for the differences in fluvial and estuarine deposit proportions between both systems.

The relatively fast transgression witnessed by the Last Interglacial TST (rates > 7 m/ka), appears to have reduced the development of organics in the system compared to the Holocene TST. Last Interglacial RSL-rise at the time of TST formation must have exceeded critical values for peat growth to keep up. Such is also to be inferred from the absence of extensive Last Interglacial palaeovalley basal peats immediately below the TST, which is in strong contrast to the slower-transgressed Holocene case. The basal peat along the rims of the Amersfoort basin to the south of the Rhine estuary (Zagwijn, 1983) are an exception within the coastal prism at large. The extensive peats in the IJssel valley basin upstream of the TST apex (Busschers et al., 2007; Peeters et al., 2016; Fig. 5), are not to be considered part of the coastal prism. Holocene basal peat occurs continuous below the TS and formed time diachronic in advance of transgression. It appears interrupted only briefly around 8.4 ka when RSL shortly accelerated to > 10 m/yr (Hijma and Cohen, 2011). Intercalated peat beds established when RSL

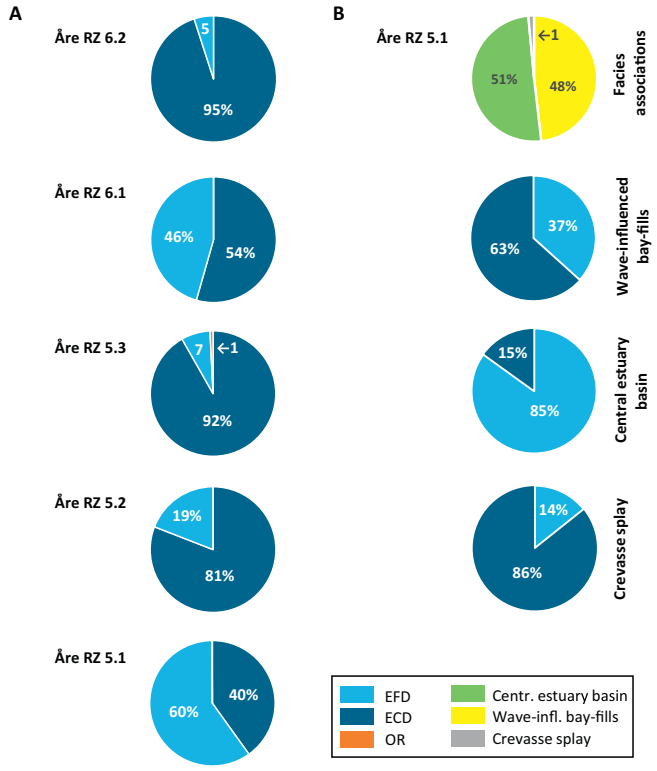

Fig. 11. A) Deposit proportions of Åre RZs 5.1–6.2. B) Deposit proportions at facies association level of Åre RZ 5.1; see Appendix B for more facies association details.

rates decelerated below 7 m/ka (e.g. Hijma et al., 2009; Bos et al., 2012; Koster et al., 2017; Van Asselen et al., 2017).

The Last Interglacial TST estuary was modestly tidally influenced, as was the Holocene TST. The lower part of the TSTs of both systems show only limited tidal indicators. The Last Interglacial tidal circulation in the North Sea is regarded similar to the Holocene situation (Beets and Van der Spek, 2000; Van der Molen and De Swart, 2001); the tidal wave into the TST estuaries was probably rapidly attenuated because of impedance by submerged sand-bars in the estuary-mouth (Hijma and Cohen, 2011; Peeters et al., 2016; De Haas et al., 2018).

Sediment delivery by the Rhine system during the Last Interglacial and the Middle Holocene alike, was mobilized and carried by discharge generated over upstream basins, weighing in the hinterland climate, vegetation cover and erodibility of source sediments. Earlier studies

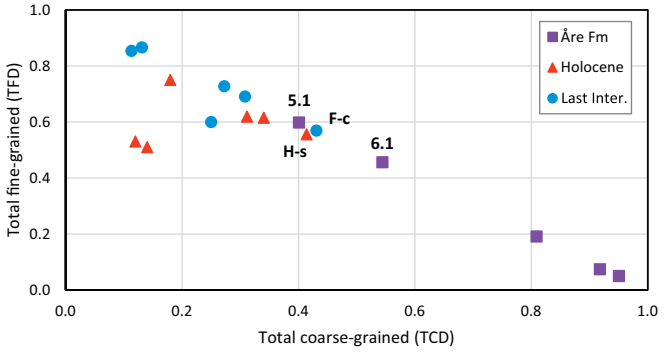

Fig. 12. Comparison of the total coarse-grained (TCD) and total fine-grained deposit (TFD) proportions of the Last Interglacial and Holocene systems, and Åre RZs 5.1–6.2. Last Interglacial segment F-c, Holocene segment H-s and Åre RZ 5.1 are indicated in the centre of the plot.

showed that during these two interglacial climatic optima, similar hinterland cover of deciduous forests had been reached (Eemian: e.g. Zagwijn, 1989, 1996; Sirocko et al., 2005; Holocene: e.g. Van Geel et al., 1981; Hoek, 1997), allowing to assume an evenly-distributed discharge-regime to explain the lower-energetic fluvial-style of the Rhine in reaches upstream of the TST apex (e.g. Berendsen and Stouthamer, 2002; Busschers et al., 2007; Peeters et al., 2015). Soil formation and the widespread occurrence of soil-protective forest vegetation during the interglacials most likely further normalized the Rhine systems, reducing sediment delivery (Berendsen et al., 1995; Erkens et al., 2011). Hence, sediment supply during the formation of both TSTs was likely similar, as is the bulk sediment-trapping rate calculated for both systems (8–9 km^3/ka), despite the differences in distribution over the depositional environments (see Section 4.3).

Based on these findings, the different initial morphology of the pre-transgressional surfaces, and the difference in RSL rise-rate - most likely owing to differences in glacio-isostatic setting (Long et al., 2015) - are regarded the key factors explaining the observed contrasts in Last Interglacial and Holocene sedimentary architecture and TST record.

5.2. Preservation of the Last Interglacial TST and HST

Two major controls determined the preservation of the Last Interglacial coastal-prism record. The first is sea-level fall following the highstand, leading to fluvial incision. It caused near-complete loss of the HST, but left significant parts of the TST to remain (Fig. 5; Fig. 8). Over longer time (> 100 ka), estuarine TSTs are likely to preserve better than deltaic HSTs, at least in the coastal prism domain. This would imply that volumetric comparisons between ancient and Quaternary records should therefore focus on TSTs. Erosion and subsequent fluvial deposition during the Weichselian glacial replaced large parts of the Last Interglacial sedimentary record in the Central Depocentre. Here, fine-grained transgressive heterolithic deposits were replaced by coarse- to medium-grained amalgamated channel-belt sands (Units A3/A5). This large-scale sediment replacement greatly changed important parameters for hydrocarbon reservoirs such as sand-body connectivity, reservoir porosity and permeability. The architecture of the Åre Formation (Fig. 7) reproduces the notions of truncation and the fines-with-coarse replacements.

The second control on preservation is valley-scale avulsion of the feeding river (e.g. Blum and Price, 1998; Slingerland and Smith, 2004; Blum and Aslan, 2006; Blum et al., 2013; Miall, 2016), which to this study's benefit, rerouted the Rhine system away from the Central Depocentre, saving the Last Interglacial sedimentary succession from further fluvial erosion. Systems occupying subsiding terrains (e.g. Po delta, Italy: Amorosi et al., 2004; Bruno et al., 2017) that do not allow for valley-scale avulsion, tend to fragmentarily preserve intercalated TST and HST units in stacked positions for which it is more difficult to identify TST-apex positions and volumetrically intercompare older and younger TSTs. Systems occupying bedrock entrenched corridors (e.g. Tagus estuary, Portugal: Vis et al., 2008, 2016; Vis and Kasse, 2009) also prevent valley avulsion, and instead preserves only patches of older TSTs as valley rim terraces, again not so favourable for detailed volumetric analysis. The Rhine case demonstrates by exception what valley-scale avulsion does for areal preservation and how important that can be in reservoir architecture creation of entire incised-valleys.

5.3. Preservation and completeness of the Åre RZs 5–6

Assessment of the applicability of the Quaternary TSTs as young analogues for the architecture of the Early Jurassic Åre Formation, first requires assessment of the preservation and completeness of Åre RZs 5–6. Significant depositional changes within the Åre Formation are in general attributed to switches between transgression and regression (Thrana et al., 2014).

The transgressive surfaces in Åre RZs 5–6 (TS2 and TS3: Fig. 7),

probably originate from the combined effect of tectonic subsidence within the Halten Terrace Basin and regional autogenic shifts of the system itself (Thrana et al., 2014). Minor hiatuses might be present at the TSs, but the biostratigraphical record lacks sufficient resolution to substantiate this. The regressive surfaces in the Åre Formation are of a completely different nature. In Åre RZs 5–6, two surfaces characterized by significant erosion were identified as candidate sequence boundaries (i.e. c.SB2 and c.SB3: Fig. 7). They mark abrupt changes in facies and depositional setting and are often characterized by field-wide distributary channel sandstones, which makes them likely to have formed in response to base-level fall. Thickness mapping shows that distributary channels cut as deep as 10 m into the underlying sediments (Thrana et al., 2014).

On a smaller scale, sets of genetically related beds of autocyclic events were most likely formed due to local autogenic shifts within the coastal system. The series of stacked upward-coarsening successions in Åre RZs 5.1 and 6.1 are interpreted to be the result of distributary channel switching within the estuarine floodbasin. These produced local transgressions and regressions in addition to local subsidence variations due to differential compaction within the heterogenous sediments (Hammer et al., 2010, 2012). Each parasequence cycle may have caused erosion of each previously deposited transgressive sequence, eventually resulting in the preservation of only the more basal parts. A low-gradient coastal plain combined with shallow water depth may have enhanced the autogenic behaviour of the system (Thrana et al., 2014).

Stratigraphic preservation and completeness of reservoir zones Åre RZs 5.1 and 6.1 follow from the reconstructed amounts of erosion (e.g. up to 10 m in Åre RZ 5.1), caused by the field-wide down-cutting of the distributary channels forming the candidate sequence boundaries (c.SB2 and c.SB3). This caused the removal of a substantial part (25–50%) of both these TSTs: a situation very similar to the one found in the central Netherlands for the Last Interglacial Rhine where c. 35% of the Last Interglacial TST volume was eroded (see Section 4.1).

Transgressive cycles in modern analogues such as in the Italian Po Plain (Amorosi et al., 2005, 2017) and the Gulf of Mexico, USA (e.g. Anderson et al., 2014; Livsey and Simms, 2016), show a cycle-duration of 1.5–2.5 ka per parasequence. Assuming that the transgressive cycles in the ancient Åre RZs 5.1 and 6.1 were of similar length - sedimentary processes and sedimentation-rates are thought not to significantly differ in ancient time from those of today (e.g. Tipper, 1983; Miall, 2015; Tipper, 2016) - periods of sedimentation presumably account for about 12-20 ka for Åre RZs 5.1 and 5–7.5 ka for Åre RZs 6.1, when calculated based on the number of preserved parasequences per RZ. If sedimentary processes and sedimentation rates in Mesozoic times were however different from the modern analogues, the parasequences would probably account for a larger portion of the deposition-duration, since one would expect accumulation rates to be lower, due to slower sea-level fluctuations which would have limited accommodation-space provision.

The deposition-duration, as calculated for Åre RZs 5.1 and 6.1, only account for a relatively small proportion (10–25%) of the estimated total duration of formation of both RZs (Fig. 7; Thrana et al., 2014). This discrepancy between expected and apparent proportion of time, might be due to internal sediment reworking and erosion in-between successive transgressive cycles, similar to examples in other stratigraphic records (e.g. Jordan et al., 2016). The large proportion of time not represented in the deposits could also be due to stasis in the sedimentary system (e.g. Miall, 2015; Tipper, 2015), characterised by non-deposition or sediment by-pass. Another cause for the discrepancy is the possibility of autogenic switching on a more extensive spatial-scale, stretching beyond the borders of the Heidrun Field (see Section 5.4 below).

5.4. Applicability potential of the Late Quaternary Rhine-records as analogue

The Late Triassic to Early Jurassic Åre Formation experienced 2nd to 3rd-order greenhouse cycles with minor fluctuations in sea level, while the Late Quaternary Rhine records were heavily influenced by high-amplitude glacio-eustasy fitting 4th-order icehouse cycles, which in addition were amplified by glacio-isostatic adjustments due to the nearby loading and unloading of the earth's crust by large ice-masses. However, despite these major differences in rates of RSL change, the Åre RZs 5 and 6 show a number of remarkable similarities in facies (proportions), preservability, autogenic processes and controlling forcings, with the Quaternary's last two TSTs in the Netherlands.

Both Åre RZs 5.1 and 6.1 experienced transgression within an estuarine flood-basin setting, forming TSTs, with erosion of the formerly deposited TST (and potentially HST) during phases of regression, leaving only the basal parts of the TSTs preserved – similar to the FSST truncation of the Last Interglacial TST (see Section 5.2). Moreover, Åre RZ 5.1, and arguably also Åre RZ 6.1, shows deposit proportions that are similar to proportions of the Last Interglacial TST (Section 4.4; Fig. 12). The overall coarser grainsize of the Åre Formation sediments would be due to its position close to the basin margin (the Norwegian mainland; Morton et al., 2009) with presumably a steep hinterland (Thrana et al., 2014), while the Rhine TST apexes are some 150-200 km away from the basin entry point (Fig. 1A).

The absence of coals in Åre RZs 5–6, as well as the absence of coastal barrier systems, by drawing simple analogues with peat absence in the Last Interglacial TST, would indicate relatively rapid drowning and an extensive provision of accommodation space, governed by high rates of RSL rise (i.e. > 7 m/ka, if not > 10 m/ka based on the Holocene counter example with peats; Section 5.1). However, this is a too simple analogue not taking the longer greenhouse versus ice-house TST durations and possible active feeder-valley position into account. In the case of the Åre Formation, large-scale avulsion processes may have resulted in lateral shifts in deposition areas and explain the parasequences observed. The main-distributary channels of Åre RZs 5.1 and 6.1 were probably part of the time active *outside* the borders of the relatively small area (16×8 km) that is now known as the Heidrun Field. The Early Jurassic palaeogeography of the eastern Halten Terrace, features several main channel belts originating from the same upland-source. Some may have co-functioned, other may have followed-up each other over time. Partial analogy can be drawn with the shift of the Rhine in the second half of the Last Glacial (Weichselian Middle Pleniglacial; Section 5.2).

The base of both Åre RZs 5.2 and 6.2 (i.e. c.SB2 and c.SB3: Fig. 7) and their truncation of respective preceding TSTs, shows similarities to the truncation of the Last Interglacial coastal prism (TST and HST) in the Netherlands. The fluvial sandstones at the base of Åre RZs 5.2 and 6.2 in this analogy resemble the valley-wide coarse-grained channel-belts of Unit A3/A5 (Fig. 5). Its erosive base features channel-lag deposits with mud clasts ripped up from the underlying TST deposits (Peeters et al., 2016), similar as recognized at the contact in Åre RZs 5.2 and 6.2. The Åre RZs 5.2 and 6.2 sandstones retained a tidally-influenced estuarine character, whereas Unit A3 marks fluvial erosion. This appears to indicate that the RSL change leading to Åre Formation c.SBs were not as large as the absolute RSL drops marking inception of Pleistocene glacials.

6. Conclusions

The unique position of both Last Interglacial and Holocene Rhine records in the Netherlands provides an excellent natural laboratory to study the stratigraphic architecture of a transgressive record that experienced one full 100-ka interglacial-glacial cycle. In this study, longitudinal trends in deposit proportions, volumes and state of preservation of the Last Interglacial and Holocene Rhine TSTs were quantitatively compared, and the applicability of such work as analogue to the reservoir geology of the Late Triassic to Early Jurassic Åre Formation off Norway was assessed.

Sedimentary volumes and deposit proportions show large differences between the Last Interglacial and Holocene TSTs. In the Holocene

record, the volume of fluvial deposits is almost six times larger and the volume of organics is almost twenty times larger than in the Last Interglacial record. Conversely, the volume of estuarine deposits in the Holocene record is only half of that of the Last Interglacial record. Still, both records developed with a remarkably similar bulk sediment-trapping rate of 8–9 km^3/ka.

The differences in architecture and composition result from (1) incised-valley configuration differences between the two depocentres and (2) the relative sea-level histories. For the Last Interglacial coastal prism, sea-level fall, and river incision and avulsion determined the amount of sediment that preserved after completion of one interglacial-glacial cycle. In the example of the Last Interglacial record, it is estimated that 40% of the original volume remained, mainly TST deposits. River avulsion at valley-scale half-way the Last Glacial prevented further erosion and reworking of the older Last Interglacial TST, which made that it can still be studied at more or less a comparable level of spatial detail as the Holocene TST.

The Last Interglacial Rhine TST deposit proportions (coarse-grained vs. fine-grained; estuarine vs. fluvial) and architectural properties show remarkable similarity with selected Early Jurassic TSTs within the Åre Formation off Norway, ranging from metre-scale vertical-successions to kilometre-scale field-wide events. From both records only the basal parts of the TSTs became preserved in the stratigraphic record. The Holocene Rhine TST lags the experience of a 100-ka interglacial-glacial cycle, which hampered its applicability as analogue. The Holocene record was nevertheless of great value to validate the Last Interglacial record for comparison with the Åre Formation and for assessment of its applicability as reservoir analogue.

Author contribution

JP: lead author, research design, geological interpretation and analysis; KMC: research design, geological interpretation; CT: specialist Åre Formation, geological interpretation; FSB: research design, geological interpretation; AWM, ES and HM: principal investigators, research design.

Acknowledgements

This study is part of the PhD research of Jan Peeters at Utrecht University and is supported by Equinor ASA, TNO-Geological Survey of the Netherlands and Deltares. Gilles Erkens (Deltares/UU), Marc Hijma (Deltares) and Marc Gouw (UU) are greatly acknowledged for discussion and access to their original research data of the Holocene Rhine. Contributions from the journal editor Adrew Miall (University of Toronto) and reviewers Alessandro Amorosi (University of Bologna) and anonymous are highly appreciated and have significantly improved this paper. The Heidrun Unit (Equinor Energy AS, ConocoPhillips Skandinavia AS, Petoro AS, Eni Norge AS) is acknowledged for permission to publish.

Color reference

For interpretation of the references to color in these figures 1, 5, 6, 7, 8, 9, 10, 11 and 12, the reader is referred to the web version of this article.

Appendix A

Table A1
A) Summary of the geometry, dominant lithology, facies and basal bounding surface of the systems tracts as recorded in the Late and Middle Pleistocene Rhine record in the Central Depocentre. Sedimentary units are cf. Peeters et al. (2016). B) Detailed geometric data of the Last Interglacial TST in segments A-c to F-c (from Peeters et al., 2016). C) Detailed geometric data of the reconstructed Last Interglacial HST in segments A-c to F-c (based on Sier et al., 2015; Peeters et al., 2016).

A. Late and Middle Pleistocene incised Rhine-valley fill - Central Depocentre

Systems Tract	Average thickness (m) - up- to downstream	Average width (km) - up- to downstream	Sedimentary unit	Dominant lithology	Sedimentary facies	Basal bounding surface
FSST	8 to 10	12 to 22	Unit A5	Gravelly, medium- to coarse-grained sands	Amalgamated channel belt	Erosive
			Unit A3	Gravelly, medium- to coarse-grained sands	Channel belt	Erosive
HST - reconstructed	0 to 7.5	11 to 22	Unit M1	Organic-rich layered clays	Estuary	Conformable
TST	2 to 14	11 to 22	Unit M1	Mollusc-rich silty clay and sands	Estuary	Conformable
			Unit A2	Organic-rich loams and silts	Flood basin	Conformable
LST	16 to 20	9.5 to 17	Unit A1	Medium to coarse-grained sands	Meandering channel belt	Conformable
			Unit S6	Gravelly, coarse-grained sands	Braided channel belt	Erosive

B. Last Interglacial TST details

Segment	F-c	E-c	D-c	C-c	B-c	A-c
Transect x-coordinate (km)	128	155	163	175	181	195
Width of segment (km) - preserved	22	12	14	15.5	10	9.5
Length of segment (km)	27	17.5	10	9	10	37

(*continued on next page*)

Table A1 (*continued*)

B. Last Interglacial TST details

Segment	F-c	E-c	D-c	C-c	B-c	A-c
Mean thickness (m) - preserved	7.5	8.0	5.5	4.8	5.5	2.0
Width of segment (km) - reconstructed	22	15	16	15.5	11	11
Mean thickness (m) - reconstr. & uncorr.	16.8	10.8	7.8	4.8	5.5	2.0

C. Last Interglacial HST details

Segment	F-c	E-c	D-c	C-c	B-c	A-c
Transect x-coordinate (km)	128	155	163	175	181	195
Width of segment (km) - reconstructed	22	15	16	15.5	11	11
Length of segment (km)	27	17.5	10	9	10	37
Mean thickness (m) - reconstr. & uncorr.	7.2	7.2	7.2	7.2	5.5	4.0

Table A2
A) Summary of the geometry, dominant lithology, facies and basal bounding surface of the systems tracts as recorded in the Holocene and Late Pleistocene Rhine record in the Southern Depocentre. Lithostratigraphic units are cf. Busschers et al. (2007), Gouw and Erkens (2007) and Hijma et al. (2009). B) Detailed geometric data of the Holocene TST in segments C-s to H-s (from Gouw and Erkens, 2007; Hijma et al., 2009).

A. Holocene and Late Pleistocene Rhine record - Southern Depocentre

Systems Tract	Average thickness (m) - up- to downstream	Average width (km) - up- to downstream	Lithostratigraphical unit	Dominant lithology	Sedimentary facies	Basal bounding surface
HST	2 to 5	15 to 55	Echteld Fm	Silty clay and clay	Flood basin	Comformable
			Echteld Fm	Sand and gravel	Channel belt	Erosive
			Naaldwijk Fm, Walcheren Mb	Undifferentiated	Undifferentiated	Mostly comformable
			Nieuwkoop Fm	Peat and gyttja	Fen (wood) peats	Comformable
TST	1.5 to 12	10 to 37	Echteld Fm	Silty clay and clay	Flood basin	Comformable
			Echteld Fm	Sand and gravel	Channel belt	Erosive
			Naaldwijk Fm, Wormer Mb	Clay with silt/very fine sand layers	Mud dominated intertidal flat	Comformable
			Naaldwijk Fm, Wormer Mb	Sand/silt with clay layers	Sand dominated intertidal flat	Comformable
LST	6 to 8	20 to 40	Kreftenheye Fm	Gravelly, coarse-grained sands	Amalgamated channel belt	Erosive

B. Holocene TST details

Segment	H-s	G-s	F-s	E-s	D-s	C-s
Transect x-coordinate (km)	85	95	105	130	145	160
Width of segment (km)	36.5	33.5	33	28	22.5	10
Length of segment (km)	10	10	17.5	20	15	15
Mean thickness (m)	12.0	9.0	7.5	4.0	2.5	1.5

Appendix B. Supplementary data

Supplementary data to this article can be found online at https://doi.org/10.1016/j.earscirev.2018.10.010.

References

Ahokas, J.M., Nystuen, J.P., Martinius, A.W., 2014. Stratigraphic signatures of punctuated rise in relative sea-level in an estuary-dominated heterolithic succession: Incised valley fills of the Toarcian Ostrealv Formation, Neill Klinter Group (Jameson Land, East Greenland). Mar. Pet. Geol. 50, 103–129.

Amorosi, A., Colalongo, M.L., Fiorini, F., Fusco, F., Pasini, G., Vaiani, S.C., Sarti, G., 2004. Palaeogeographic and palaeoclimatic evolution of the Po Plain from 150-ky core records. Glob. Planet. Chang. 40, 55–78.

Amorosi, A., Centineo, M.C., Colalongo, M.L., Fiorini, F., 2005. Millenial-scale depositional cycles from the Holocene of the Po Plain, Italy. Mar. Geol. 222-223, 7–18.

Amorosi, A., Bruno, L., Campo, B., Morelli, A., Rossi, V., Scarponi, D., Hong, W., Bohacs, K.M., Drexler, T.M., 2017. Global sea-level control on local parasequence architecture from the Holocene record of the Po Plain, Italy. Mar. Pet. Geol. 87, 99–111.

Anderson, J.B., Wallace, D.J., Simms, A.R., Rodriguez, A.B., Milliken, K.T., 2014. Variable response of coastal environments of the northwestern Gulf of Mexico to sea-level rise and climate change: Implications for future change. Mar. Geol. 352, 348–366.

Aschof, J.L., Olariu, C., Steel, R.J., 2018. Recognition and significance of bayhead delta deposits in the rock record: A comparison of modern and ancient systems.

Sedimentology 65, 62–95.
Bachu, S., 2008. CO_2 storage in geological media: Role, means, status and barriers to deployment. Prog. Energy Combust. Sci. 34, 254–273.
Barlow, N.L.M., McClymont, E.L., Whitehouse, P.L., Stokes, C.R., Jamieson, S.S.R., Woodroffe, S.A., Bentley, M.J., Callard, S.L., Ó Cofaigh, C., Evans, D.J.A., Horrocks, J.R., Lloyd, J.M., Long. A.J., Margold, M., Roberts, D.H., Sanchez-Montes, M.L., 2018. Lack of evidence for a substantial sea-level fluctuation within the Last Interglacial. Nat. Geosci. 11, 627–634.
Bassinot, F.C., Labeyrie, L.D., Vincent, E., Quidelleur, X., Shackleton, N.J., Lancelot, Y., 1994. The astronomical theory of climate and the age of the Brunhes-Matuyama magnetic reversal. Earth Planet. Sci. Lett. 126, 91–108.
Beets, D.J., Van der Spek, A.J.F., 2000. The Holocene evolution of the barrier and back-barrier basins of Belgium and the Netherlands as a function of late Weichselian morphology, relative sea-level rise and sediment supply. Neth. J. Geosci. 79, 3–16.
Beets, D.J., De Groot, T.A.M., Davies, H.A., 2003. Holocene tidal back-barrier development at decelerating sea-level rise: a 5 millennia record, exposed in the western Netherlands. Sediment. Geol. 158, 117–144.
Bentley Sr., S.J., Blum, M.D., Maloney, J., Pond, L., Paulsell, R., 2016. The Mississippi River source-to-sink system: Perspectives on tectonic, climatic, and anthropogenic influences, Miocene to Anthropocene. Earth Sci. Rev. 153, 139–174.
Berendsen, 1982. De genese van het landschap in het zuiden van de provincie Utrecht: een fysisch-geografische studie. PhD thesis, Utrecht University. Utrechtse Geografische studies 10.
Berendsen, H.J.A., Stouthamer, E., 2000. Late Weichselian and Holocene palaeogeography of the Rhine-Meuse delta, The Netherlands. Palaeogeogr. Palaeoclimatol. Palaeoecol. 161, 311–335.
Berendsen, H.J.A., Stouthamer, E., 2002. Paleogeographic evolution and avulsion history of the Holocene Rhine-Meuse delta, The Netherlands. Neth. J. Geosci. 81, 97–112.
Berendsen, H.J.A., Hoek, W.Z., Schorn, E.A., 1995. Late Weichselian and Holocene river channel changes of the Rivers Rhine and Meuse in the Netherlands (Land van Maas en Waal). Paläoklimaforschung 14, 151–171.
Bjørlykke, K., Jahren, J., Aagaard, P., Fisher, Q., 2010. Role of effective permeability distribution in estimating overpressure using basin modelling. Mar. Pet. Geol. 27, 1684–1691.
Blum, M.D., Aslan, A., 2006. Signatures of climate vs. sea-level change within incised valley-fill successions: Quaternary examples from the Texas Gulf Coast. Sediment. Geol. 190, 177–211.
Blum, M.D., Price, D.M., 1998. Quaternary alluvial plain construction in response to glacio-eustatic and climatic controls, Texas Gulf Coastal Plain. In: Shanley, K.W., McCabe, P.J. (Eds.), Relative Role of Eustasy. Climate and Tectonism in Continental Rocks, SEPM Special Publication Vol. 59. pp. 31–48.
Blum, M.D., Törnqvist, T.E., 2000. Fluvial responses to climate and sea-level change: a review and look forward. Sedimentology 47, 2–48.
Blum, M.D., Martin, J., Milliken, K., Garvin, M., 2013. Paleovalley systems: Insights from Quaternary analogs and experiments. Earth Sci. Rev. 116, 128–169.
Bos, I.J., Stouthamer, E., 2011. Spatial and temporal distribution of sand-containing basin fills in the Holocene Rhine-Meuse delta, the Netherlands. The Journal of Geology 119, 641–660.
Bos, I.J., Busschers, F.S., Hoek, W.Z., 2012. Organic-facies determination: a key for understanding facies distribution in the basal peat layer of the Holocene Rhine-Meuse delta, The Netherlands. Sedimentology 59, 679–703.
Brewer, S., Guiot, J., Sánchez-Goñi, M.F., Klotz, S., 2008. The climate in Europe during the Eemian: a multi-method approach using pollen data. Quat. Sci. Rev. 27, 2303–2315.
Bruno, L., Amorosi, A., Severi, P., Costagli, B., 2017. Late Quaternary aggradation rates and stratigraphic architecture of the southern Po Plain, Italy. Basin Res. 29, 234–248.
Busschers, F.S., Weerts, H.J.T., Wallinga, J., Cleveringa, P., Kasse, C., De Wolf, H., Cohen, K.M., 2005. Sedimentary architecture and optical dating of Middle and Late Pleistocene Rhine-Meuse deposits - fluvial response to climate change, sea-level fluctuation and glaciation. Neth. J. Geosci. 84, 25–41.
Busschers, F.S., Kasse, C., Van Balen, R.T., Vandenberghe, J., Cohen, K.M., Weerts, H.J.T., Wallinga, J., Johns, C., Cleveringa, P., Bunnik, F.P.M., 2007. Late Pleistocene evolution of the Rhine-Meuse system in the southern North Sea basin: imprints of climate change, sea-level oscillation and glacio-isostasy. Quat. Sci. Rev. 26, 3216–3248.
Busschers, F.S., Van Balen, R.T., Cohen, K.M., Kasse, C., Weerts, H.J.T., Wallinga, J., Bunnik, F.P.M., 2008. Response of the Rhine-Meuse fluvial system to Saalian ice-sheet dynamics. Boreas 37, 377–398.
Cattaneo, A., Steel, R.J., 2003. Transgressive deposits: a review of their variability. Earth Sci. Rev. 62, 187–228.
Cohen, K.M., 2003. Differential subsidence within a coastal prism - Late-Glacial – Holocene tectonics in the Rhine-Meuse delta. the Netherlands. PhD thesis, Utrecht University. Nederlandse Geografische Studies, pp. 316.
Cohen, K.M., Hijma, M.P., 2014. The Transgressive Early-Middle Holocene Boundary: The Case for a GSSP at Rotterdam, Rhine Delta, North Sea Basin. In: Rocha R., Pais, J., Kullberg, J.C., Finney, S. (Eds.), STRATI 2013, Springer Geology, pp. 925–929.
Cohen, K.M., Stouthamer, E., Berendsen, H.J.A., 2002. Fluvial deposits as a record for Late Quaternary neotectonic activity in the Rhine-Meuse delta, The Netherlands. Neth. J. Geosci. 81 (3–4), 389–405.
Dalland, A., Worsley, D., Ofstad, K., 1988. A lithostratigraphic scheme for the Mesozoic and Cenozoic succession offshore mid- and northern Norway. Bulletin of the Norwegian Petroleum Directorate 4, 1–65.
Dalrymple, R.W., 2006. Incised valleys in time and space: An introduction to the volume and an examination of the controls on valley formation and filling. In: Dalrymple, R.W., Leckie, D.A., Tillman, R.W. (Eds.), Incised Valleys in Time and Space. SEPM Special Publication Vol. 85. pp. 5–12.
De Haas, T., Pierik, H.J., Van der Spek, A.J.F., Cohen, K.M., Van Maanen, B., Kleinhans, M.G., 2018. Holocene evolution of tidal systems in The Netherlands: Effects of rivers, coastal boundary conditions, eco-engineering species, inherited relief and human interference. Earth Sci. Rev. 177, 139–163.
Dutton, A., Lambeck, K., 2012. Ice volume and sea level during the Last Interglacial. Science 337, 216–219.
Erkens, G., 2009. Sediment dynamics in the Rhine catchment: quantification of fluvial response to climate change and human impact. PhD thesis, Utrecht University. Netherlands Geographical Studies 388.
Erkens, G., Cohen, K.M., 2009. Quantification of intra-Holocene sedimentation in the Rhine-Meuse delta: a record of variable sediment delivery. In: Erkens, G. (Ed.), Sediment dynamics in the Rhine catchment: quantification of fluvial response to climate change and human impact. PhD thesis, Utrecht University. Netherlands Geographical Studies 388, pp. 117–171.
Erkens, G., Hoffmann, T., Gerlach, R., Klostermann, J., 2011. Complex fluvial response to Lateglacial and Holocene allogenic forcing in the Lower Rhine Valley (Germany). Quat. Sci. Rev. 30, 611–627.
Erkens, G., Van der Meulen, M.J., Middelkoop, H., 2016. Double trouble: subsidence and CO_2 respiration due to 1,000 years of Dutch coastal peatlands cultivation. Hydrogeol. J. 24, 551–568.
Gouw, M.J.P., 2008. Alluvial architecture of the Holocene Rhine-Meuse delta (the Netherlands). Sedimentology 55, 1487–1516.
Gouw, M.J.P., Berendsen, H.J.A., 2007. Variability of channel-belt dimensions and the consequences for alluvial architecture: observations from the Holocene Rhine-Meuse delta (The Netherlands) and Lower Mississippi Valley (U.S.A.). J. Sediment. Res. 77, 124–138.
Gouw, M.J.P., Erkens, G., 2007. Architecture of the Holocene Rhine-Meuse delta (the Netherlands) – A result of changing external controls. Neth. J. Geosci. 86-1, 23–54.
Hammer, E., Mørk, M.B.E., Næss, A., 2010. Facies controls on the distribution of diagenesis and compaction in fluvial-deltaic deposits. Mar. Pet. Geol. 27, 1737–1751.
Hammer, E., Brandsegg, K.B., Mørk, M.B.E., Næss, A., 2012. Reconstruction of heterogeneous reservoir architecture based on differential decompaction in sequential reburial modelling. Pet. Geosci. 18, 173–189.
Hangx, S., Bakker, E., Bertier, P., Nover, G., Busch, A., 2015. Chemical-mechanical coupling observed for depleted oil reservoirs subjected to long-term CO_2-exposure – A case study of the Werkendam natural CO_2 analogue field. Earth Planet. Sci. Lett. 428, 230–242.
Haq, B.U., Hardenbol, J., Vail, P.R., 1987. Chronology of fluctuating sea levels since the Triassic. Science 235, 1156–1166.
Haq, B.U., Hardenbol, J., Vail, P.R., 1988. Mesozoic and Cenozoic chronostratigraphy and cycles of sea-level change. In: Wilgus, C.K., Hastings, B.S., Kendall, C.G.St.C., Posamentier, H.W., Ross, C.A., Van Wagoner, J.C. (Eds.), Sea Level Changes: An Integrated Approach. SEPM Special Publication Vol. 42. pp. 71–108.
Haszeldine, R.S., 2009. Carbon capture and storage: How green can black be? Science 325, 1647–1652.
Hijma, M.P., Cohen, K.M., 2010. Timing and magnitude of the sea-level jump preluding the 8200 yr event. Geology 38, 275–278.
Hijma, M.P., Cohen, K.M., 2011. Holocene transgression of the Rhine river mouth area, The Netherlands/Southern North Sea: palaeogeography and sequence stratigraphy. Sedimentology 58, 1453–1485.
Hijma, M.P., Cohen, K.M., Hoffmann, G., Van der Spek, A.J.F., Stouthamer, E., 2009. From river valley to estuary: the evolution of the Rhine mouth in the early to middle Holocene (western Netherlands, Rhine-Meuse delta). Neth. J. Geosci. 88, 13–53.
Hijma, M.P., Van der Spek, A.J.F., Van Heteren, S., 2010. Development of a mid-Holocene estuarine basin, Rhine-Meuse mouth area, offshore The Netherlands. Mar. Geol. 271, 198–211.
Hijma, M.P., Cohen, K.M., Roebroeks, W., Westerhoff, W.E., Busschers, F.S., 2012. Pleistocene Rhine-Thames landscapes: geological background for hominin occupation of the southern North Sea region. J. Quat. Sci. 27, 17–29.
Hoek, W.Z., 1997. Late-glacial and early Holocene climatic events and chronology of vegetation development in the Netherlands. Veg. Hist. Archaeobotany 6, 197–213.
Howell, J.A., Martinius, A.W., Good, T.R., 2014. The application of outcrop analogues in geological modelling: a review, present status and future outlook. In: Martinius, A.W., Howell, J.A., Good, T.R. (Eds.), Sediment-Body Geometry and Heterogeneity: Analogue studies for Modelling the Subsurface. Geological Society, London, Special Publications Vol. 387. pp. 1–25.
Jordan, O.D., Gupta, S., Hampson, G.J., Johnson, H.D., 2016. Preserved stratigraphic architecture and evolution of a net-transgressive mixed wave- and tide-influenced coastal system: The Cliff House sandstone northwestern New Mexico, U.S.A. J. Sediment. Res. 86, 1399–1424.
Kjærefjord, J.M., 1999. Bayfill successions in the Lower Jurassic Åre Formation, Offshore Norway: Sedimentology and heterogeneity based on subsurface data from the Heidrun field and analogue data from the Upper Cretaceous Neslen Formation, Eastern Book Cliffs. Utah. GCSSEPM Foundation 19th Annual Research Conference, pp. 149–158.
Kombrink, H., Bridge, J.S., Stouthamer, E., 2007. The alluvial architecture of the Coevorden Field (Upper Carboniferous), the Netherlands. Neth. J. Geosci. 86, 3–14.
Koster, K., Stafleu, J., Cohen, K.M., 2017. Generic 3D interpolation of Holocene base-level rise and provision of accommodation space, developed for the Netherlands coastal plain and infilled palaeovalleys. Basin Res. 29, 775–797.
Leren, B.L.S., Howell, J., Enge, H., Martinius, A.W., 2010. Controls on stratigraphic architecture in contemporaneous delta systems from the Eocene Roda Sandstone, Tremp-Graus Basin, northern Spain. Sediment. Geol. 229, 9–40.
Livsey, D., Simms, A.R., 2016. Episodic flooding of estuarine environments in response to drying climate over the last 6000 years in Baffin Bay, Texas. Mar. Geol. 381, 142–162.
Long, A.J., Barlow, N.L.M., Busschers, F.S., Cohen, K.M., Gehrels, W.R., Wake, L.M., 2015.

Near-field sea-level variability in northwest Europe and ice sheet stability during the last interglacial. Quat. Sci. Rev. 126, 26–40.
Marsh, N., Imber, J., Holdsworth, R.E., Brockbank, P., Ringrose, P., 2010. The structural evolution of the Halten Terrace, off-shore Mid-Norway: extensional fault growth and strain locations in a multi-layer brittle-ductile system. Basin Res. 22, 196–214.
Martinius, A.W., Gowland, S., 2011. Tide-influenced fluvial bedforms and tidal bore deposits (Late Jurassic Lourinhã Formation, Lusitanian Basin, Western Portugal). Sedimentology 58, 285–324.
Martinius, A.W., Van den Berg, J.H., 2011. Atlas of Sedimentary Structures in Estuarine and Tidally-influenced River Deposits of the Rhine-Meuse-Scheldt System: Their Application to the Interpretation of Analogous Outcrop and Subsurface Depositional Systems. EAGE Publications, Houten, The Netherlands.
Martinius, A.W., Kaas, I., Næss, A., Helgesen, G., Kjærefjord, J.M., Leith, D.A., 2001. Sedimentology of the heterolithic and tide-dominated Tilje Formation (Early Jurassic, Halten Terrace, offshore mid-Norway). In: Martinsen, O.J., Dreyer, T. (Eds.), Sedimentary environments offshore Norway – Palaeozoic to recent. NPF Special Publication Vol. 10. pp. 103–144.
Martinius, A.W., Ringrose, P.S., Brostrøm, C., Elfenbein, C., Næss, A., Ringås, J.E., 2005. Reservoir challenges of heterolithic tidal sandstone reservoirs in the Halten Terrace, mid-Norway. Pet. Geosci. 11, 3–16.
Medina-Elizalde, M., 2013. A global compilation of coral sea-level benchmarks: Implications and new challenges. Earth Planet. Sci. Lett. 362, 310–318.
Messina, C., Nemec, W., Martinius, A.W., Elfenbein, C., 2014. The Garn Formation (Bajocian-Bathonian) in the Kristin Field, Halten Terrace: its origin, facies architecture and primary heterogeneity model. In: Martinius, A.W., Ravnås, R., Howell, J.A., Steel, R.J., Wonham, J.P. (Eds.), From Depositional Systems to Sedimentary Successions on the Norwegian Continental Margin. International Association of Sedimentologists, Special Publication Vol. 46. pp. 513–550.
Miall, A.D., 2015. Updating uniformitarianism: stratigraphy as just a set of 'frozen accidents'. In: Smith, D.G., Bailey, R.J., Burgess, P., Fraser, A. (Eds.), Strata and time: probing the gaps in our understanding. Geological Society, London, Special Publications Vol. 404. pp. 11–36.
Miall, A.D., 2016. The valuation of unconformities. Earth Sci. Rev. 163, 22–71.
Mitchum Jr., R.M., Van Wagoner, J.C., 1990. High-frequency sequences and eustatic cycles in the Gulf of Mexico basin. Proceedings, Gulf Coast Section SEPM 11th Annual Research conference. pp. 257–267.
Morton, A., Hallsworth, C., Strogen, D., Whitham, A., Fanning, M., 2009. Evolution of provenance in the NE Atlantic rift: The Early-Middle Jurassic succession in the Heidrun Field, Halten Terrace, offshore Mid-Norway. Mar. Pet. Geol. 26, 1100–1117.
Peeters, J., Busschers, F.S., Stouthamer, E., 2015. Fluvial evolution of the Rhine during the last interglacial-glacial cycle in the southern North Sea basin: A review and look forward. Quat. Int. 357, 176–188.
Peeters, J., Busschers, F.S., Stouthamer, E., Bosch, J.H.A., Van den Berg, M.W., Wallinga, J., Versendaal, A.J., Bunnik, F.P.M., Middelkoop, H., 2016. Sedimentary architecture and chronostratigraphy of a late Quaternary incised-valley fill: A case study of the late Middle and Late Pleistocene Rhine system in the Netherlands. Quat. Sci. Rev. 131, 211–236.
Pierik, H.J., Cohen, K.M., Vos, P.C., Van der Spek, A.J.F., Stouthamer, E., 2017. Late Holocene coastal-plain evolution of the Netherlands: the role of natural preconditions in human-induced sea ingressions. Proc. Geol. Assoc. 128, 180–197.
Posamentier, H.W., Jervey, M.T., Vail, P.R., 1988. Eustatic controls on clastic deposition, I: Conceptual framework. In: Wilgus, C.K., Hastings, B.S., Kendall, C.G.St.C., Posamentier, H.W., Ross, C.A., Van Wagoner, J.C. (Eds.), Sea Level Changes: An Integrated Approach. SEPM Special Publication Vol. 42. pp. 110–124.
Sier, M.J., Peeters, J., Dekkers, M.J., Parés, J.M., Chang, L., Busschers, F.S., Wallinga, J., Cohen, K.M., Bunnik, F.P.M., Roebroeks, W., 2015. The Blake Event record near the Eemian type locality – A diachronic onset of the Eemian in Europe. Quat. Geochronol. 28, 12–28.
Sirocko, F., Seelos, K., Schaber, K., Rein, B., Dreher, F., Diehl, M., Lehne, R., Jäger, K., Krbetschek, M., Degering, D., 2005. A late Eemian aridity pulse in central Europe during the last glacial inception. Nature 436, 833–836.
Slingerland, R., Smith, N.D., 2004. River avulsions and their deposits. Annu. Rev. Earth Planet. Sci. 32, 257–285.
Stouthamer, E., Cohen, K.M., Gouw, M.J.P., 2011. Avulsion and its implications for fluvial–deltaic architecture: insights from the Holocene Rhine–Meuse delta. In: Davidson, S.K., Leleu, S., North, C.P. (Eds.), From River to Rock Record: The Preservation of Fluvial Sediments and Their Subsequent Interpretation. SEPM Special Publication Vol. 97. pp. 215–232.
Thrana, C., Næss, A., Leary, S., Gowland, S., Brekken, M., Taylor, A., 2014. Updated depositional and stratigraphic model of the Lower Jurassic Åre Formation, Heidrun Field, Norway. In: Martinius, A.W., Ravnås, R., Howell, J.A., Steel, R.J., Wonham, J.P. (Eds.), From Depositional Systems to Sedimentary Successions on the Norwegian Continental Margin. International Association of Sedimentologists, Special Publication Vol. 46. pp. 253–290.
Tipper, J.C., 1983. Rates of sedimentation, and stratigraphical completeness. Nature 302, 696–698.
Tipper, J.C., 2015. The importance of doing nothing: stasis in sedimentation systems and its stratigraphic effects. In: Smith, D.G., Bailey, R.J., Burgess, P.M., Fraser, A.J. (Eds.), Strata and time: Probing the gaps in our understanding. Geological Society, London, Special Publications Vol. 404. pp. 105–122.
Tipper, J.C., 2016. Measured rates of sedimentation: What exactly are we estimating and why? Sediment. Geol. 339, 151–171.
TNO-GSN, 2016. Geological Survey of the Netherlands. TNO-GSN subsurface database at DINOloket (Data and Information on the Dutch Subsurface). (Data retrieved on [31-01-2016] from). http://www.dinoloket.nl.
Törnqvist, T.E., 1993. Fluvial sedimentary geology and chronology of the Holocene Rhine-Meuse delta, the Netherlands. PhD thesis, Utrecht University. Netherlands Geographical Studies 166.
Törnqvist, T.E., Wallinga, J., Murray, A.S., De Wolf, H., Cleveringa, P., De Gans, W., 2000. Response of the Rhine-Meuse system (west-central Netherlands) to the last Quaternary glacio-eustatic cycles: a first assessment. Glob. Planet. Chang. 27, 89–111.
Törnqvist, T.E., Wallinga, J., Busschers, F.S., 2003. Timing of the last sequence boundary in a fluvial setting near the highstand shoreline – insights from optical dating. Geology 31, 279–282.
Van Asselen, S., Cohen, K.M., Stouthamer, E., 2017. The impact of avulsion on groundwater level and peat formation in delta floodbasins during the middle-Holocene transgression in the Rhine-Meuse delta, The Netherlands. The Holocene 27, 1694–1706.
Van Balen, R.T., Houtgast, R.F., Cloetingh, S.A.P.L., 2005. Neotectonics of The Netherlands: a review. Quat. Sci. Rev. 24, 439–454.
Van den Berg, M.W., Beets, D.J., 1987. Saalian glacial deposits and morphology in The Netherlands. In: Van der Meer, J.J.M. (Ed.), Tills and Glaciotectonics. Balkema, Rotterdam, pp. 235–251.
Van der Molen, J., De Swart, H.E., 2001. Holocene tidal conditions and tide-induced sand transport in the southern North Sea. J. Geophys. Res. 106, 9339–9362.
Van der Woude, J.D., 1984. The fluviolagoonal palaeoenvironment in the Rhine/Meuse deltaic plain. Sedimentology 31, 395–400.
Van Geel, B., Bohncke, S.J.P., Dee, H., 1981. A palaeoecological study of an upper Late Glacial and Holocene sequence from "De Borchert", The Netherlands. Rev. Palaeobot. Palynol. 31, 367–448.
Van Leeuwen, R.J.W., Beets, D.J., Bosch, J.H.A., Burger, A.W., Cleveringa, P., Van Harten, D., Waldemar Herngreen, G.F., Kruk, R.W., Langereis, C.G., Meyer, T., Pouwer, R., De Wolf, H., 2000. Stratigraphy and integrated facies analysis of the Saalian and Eemian deposits in the Amsterdam-Terminal borehole, the Netherlands. Neth. J. Geosci. 79, 161–196.
Van Wagoner, J.C., Posamentier, H.W., Mitchum, R.M., Vail, P.R., Sarg, J.F., Loutit, T.S., Hardenbol, J., 1988. An overview of the fundamentals of sequence stratigraphy and key definitions. In: Wilgus, C.K., Hastings, B.S., Kendall, C.G.St.C., Posamentier, H.W., Ross, C.A., Van Wagoner, J.C. (Eds.), Sea Level Changes: An Integrated Approach. SEPM Special Publication Vol. 42. pp. 39–45.
Van Wagoner, J.C., Mitchum, R.M., Campion, K.M., Rahmanian, V.D., 1990. Siliciclastic sequence stratigraphy in well logs, cores and outcrops: Concepts for high resolution correlations of time and facies. In: AAPG, Methods in Exploration 7. U.S.A, Tulsa.
Vis, G.-J., Kasse, C., 2009. Late Quaternary valley-fill succession of the Lower Tagus Valley, Portugal. Sediment. Geol. 221, 19–39.
Vis, G.-J., Kasse, C., Vandenberghe, J., 2008. Late Pleistocene and Holocene palaeogeography of the Lower Tagus Valley (Portugal): effects of relative sea level, valley morphology and sediment supply. Quat. Sci. Rev. 27, 1682–1709.
Vis, G.-J., Kasse, C., Kroon, D., Vandenberghe, J., Jung, S., Lebreiro, S.M., Rodrigues, T., 2016. Time-integrated 3D approach of late Quaternary sediment-depocentre migration in the Tagus depositional system: from river valley to abyssal plain. Earth-Sci. Rev. 153, 192–211.
Vos, P.C., 2015. Origin of the Dutch coastal landscape: Long-term landscape evolution of the Netherlands during the Holocene, described and visualised in national, regional and local palaeogeographical map series. PhD thesis, Utrecht University.
Vos, P.C., Bunnik, F.P.M., Cohen, K.M., Cremer, H., 2015. A staged geogenetic approach to underwater archaeological prospection in the Port of Rotterdam (Yangtzehaven, Maasvlakte, The Netherlands): A geological and palaeoenvironmental case study for local mapping of Mesolithic lowland landscapes. Quat. Int. 367, 4–31.
Waelbroeck, C., Labeyrie, L., Michel, E., Duplessy, J.C., McManus, J.F., Lambeck, K., Balbon, E., Labracherie, M., 2002. Sea-level and deep-water temperature changes derived from benthic foraminifera isotopic records. Quat. Sci. Rev. 21, 295–305.
Wallinga, J., Törnqvist, T.E., Busschers, F.S.B., Weerts, H.J.T., 2004. Allogenic forcing of the Late Quaternary Rhine-Meuse fluvial record: the interplay of sea-level change, climate change and crustal movements. Basin Res. 16, 535–547.
Zagwijn, W.H., 1961. Vegetation, climate and radiocarbon datings in the Late Pleistocene of The Netherlands, Part I: Eemian and Early Weichselian. Mededelingen Geologische Stichting 14, 15–45.
Zagwijn, W.H., 1983. Sea-level changes in The Netherlands during the Eemian. Geologie en Mijnbouw / Netherlands Journal of Geosciences 62, 437–450.
Zagwijn, W.H., 1989. Vegetation and climate during warmer intervals in the Late Pleistocene of western and central Europe. Quat. Int. 3 (4), 57–67.
Zagwijn, W.H., 1996. An analysis of Eemian climate in Western and Central Europe. Quat. Sci. Rev. 15, 451–469.
Ziegler, P.A., 1994. Cenozoic rift system of western and central Europe: an overview. Geologie en Mijnbouw / Netherlands Journal of Geosciences 73, 99–127.